

Vine copula mixture models and clustering for non-Gaussian data

Özge Sahin^{a,*}, Claudia Czado^{a,b}

^a*Department of Mathematics, Technische Universität München, Boltzmanstraße 3, 85748 Garching, Germany*

^b*Munich Data Science Institute, Walther-von-Dyck-Straße 10, 85748 Garching, Germany*

Abstract

The majority of finite mixture models suffer from not allowing asymmetric tail dependencies within components and not capturing non-elliptical clusters in clustering applications. Since vine copulas are very flexible in capturing these dependencies, a novel vine copula mixture model for continuous data is proposed. The model selection and parameter estimation problems are discussed, and further, a new model-based clustering algorithm is formulated. The use of vine copulas in clustering allows for a range of shapes and dependency structures for the clusters. The simulation experiments illustrate a significant gain in clustering accuracy when notably asymmetric tail dependencies or/and non-Gaussian margins within the components exist. The analysis of real data sets accompanies the proposed method. The model-based clustering algorithm with vine copula mixture models outperforms others, especially for the non-Gaussian multivariate data.

Keywords: Dependence, ECM algorithm, model-based clustering, multivariate finite mixtures, pair-copula, statistical learning

1. Introduction

Finite mixture models are convenient statistical tools for model-based clustering. They assume that observations in the multivariate data can be clustered using k components. Each component has its density, and each observation is assigned to a component with a probability. They have many applications in finance, genetics, and marketing (e.g., Hu (2006); Gambacciani & Paoella (2017); Sun et al. (2017); Zhang & Shi (2017)). McLachlan & Peel (2000) provides more details about the finite mixture models. Both Bouveyron & Brunet-Saumard (2014) and McNicholas (2016) review recent model-based clustering methods.

One of the main questions to be addressed in the finite mixture models is *how to select the density of each component*. An early answer to this question is to assume a symmetric distribution such as multivariate normal distribution (e.g., Celeux & Govaert (1995); Fraley & Raftery (1998)) or multivariate t distribution (e.g., Peel & McLachlan (2000); Andrews & McNicholas (2011)). However, these models cannot accommodate the shape of asymmetric components. Hennig (2010) showed one such data example. Their skewed

*Corresponding author

Email addresses: ozge.sahin@tum.de (Özge Sahin), cczado@ma.tum.de (Claudia Czado)

formulations and factor analyzers, therefore, have been extensively studied (e.g., [Lin et al. \(2007\)](#); [Lee & McLachlan \(2014\)](#); [Murray et al. \(2017\)](#)).

Additionally, the models based on other distributions, for example, shifted asymmetric Laplace distributions ([Franczak et al. \(2014\)](#)), multivariate power exponential distributions ([Dang et al. \(2015\)](#)), and generalized hyperbolic distributions ([Browne & McNicholas \(2015\)](#)) have been proposed for the past few years. Since one of the main interests of copulas is to relax the normality assumption both in marginal distributions and dependence structure, the finite mixture models with copulas have also been studied (e.g., [Diday & Vrac \(2005\)](#); [Kosmidis & Karlis \(2016\)](#); [Zhuang et al. \(2021\)](#)). [Cuvelier & Fraiture \(2005\)](#) worked with the Clayton copula to represent lower tail dependence within the components, while [Vrac et al. \(2005\)](#) applied the Frank copula to have non-Gaussian but symmetric dependence. Nevertheless, these methods raise another question in the finite mixture models: *how to select flexible densities of each component so the model can represent different asymmetric or/and tail dependencies for different pairs of variables*. For this question, the vine copula or pair copula construction is a flexible and efficient tool in high-dimensional dependence modeling ([Joe \(1996\)](#); [Aas et al. \(2009\)](#)).

For illustration, consider a data set simulated from a mixture of two three-dimensional vine copulas shown in [Figure 1](#). Its data generating process includes asymmetric tail and non-Gaussian dependencies in the components. Most univariate margins are chosen to be non-Gaussian and heavy-tailed. As seen in the top left panel of [Figure 1](#), the components are well separated on two out of three bivariate scatter plots. Marginal multimodality can be seen for the second variable. The resulting components are non-elliptical, similar to a banana shape, as shown in the top right. After fitting a mixture of multivariate normal distributions with two components, its challenge to capture the true shape of the components can be seen in the bottom left panel, where the associated Bayesian Information Criterion (BIC) ([Schwarz, 1978](#)) and misclassification rate are provided. Even though fitting a mixture of multivariate skew t distributions with two components in the bottom right provides a better fit than the mixture of multivariate normal distributions fit, it can also not reveal the true characteristics of the data set. The mixture of multivariate normal distributions and multivariate skew t distributions is fitted using the R packages `mclust` ([Scrucca et al., 2016](#)) and `mixsmsn` ([Prates et al., 2013](#)), respectively. The fitting procedures apply 100 different seeds and report the best performance in terms of the misclassification rate.

To capture such behavior, applying the vine copula in finite mixture models has been explored before (e.g., [Kim et al. \(2013\)](#); [Roy & Parui \(2014\)](#); [Weiß & Scheffer \(2015\)](#); [Sun et al. \(2017\)](#)). However, they only worked with a subclass of vine tree structures and a small number of pair copula families. Therefore, a vine copula mixture model with all classes of vine tree structures and many different pair copula families is needed. Since it provides flexible densities, formulating its model-based clustering algorithm overcomes the drawbacks mentioned above, especially for non-Gaussian data.

In this paper, we formulate a vine copula mixture model for continuous data allowing all types of vine

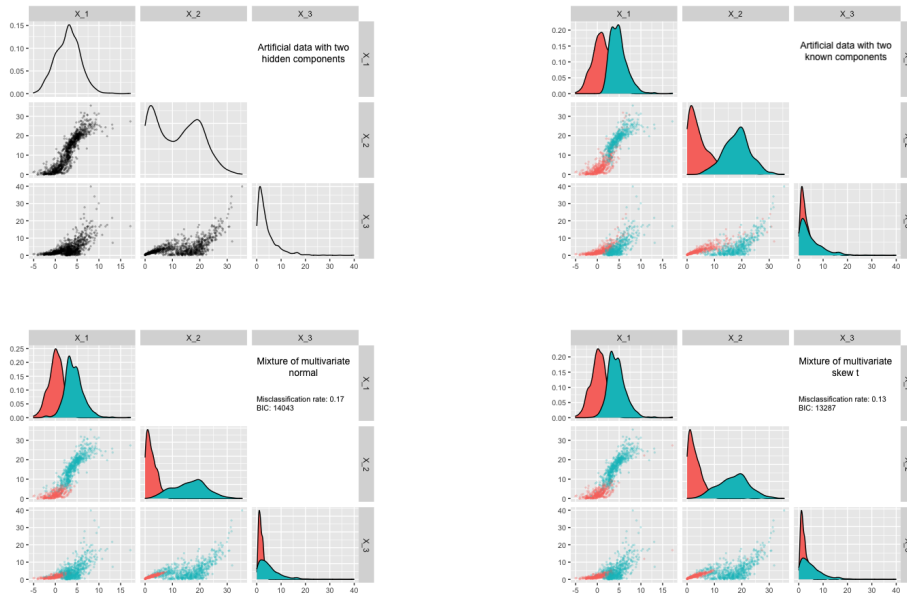


Figure 1: Pairwise scatter plot of a simulated data set (500 observations per component) under the scenario specified in Figure 4 and Table 1 (top left). The red and green points show the observations of one cluster and the other cluster (top right), respectively. The bottom left and bottom right plots display the fitted mixture of multivariate normal and multivariate skew t distributions, respectively. The diagonal of the plots gives the fitted marginal density function for each component.

tree structures, parametric pair copulas, and margins. For simplicity, we treat the number of components as known and present well-performing solutions for the remaining model selection problems. We adopt the expectation conditional maximum algorithm for parameter estimation. The paper is the first study in the finite mixture models literature that works with the full class of vine tree structures and a wide range of pair copula families to the best of the authors' knowledge. It combines the flexibility of vine copulas and finite mixture models to capture complex and diverse dependence structures in the multivariate data. Another contribution of the paper is a new model-based clustering algorithm, called *VCMM*, that incorporates realistic interdependence structures of clusters. *VCMM* is interpretable and allows for various shapes of the clusters. It shows how the dependence structure varies within clusters of the data.

The remainder of the paper is organized as follows. Section 2 gives an overview of vine copulas. Section 3 and Section 4 describe the vine copula mixture model and the new model-based clustering algorithm based on it. Simulation studies and analysis of real data are presented in Sections 5 and 6. Section 7 discusses our results and concludes the paper.

2. Vine copulas

In this section, we will recall some essential concepts of vine copulas. For more details, we refer to Chapter 3 of Joe (2014), Aas et al. (2009), and Czado (2019).

A d -dimensional copula C is a multivariate distribution on the unit hypercube $[0, 1]^d$ with univariate uniform margins. Vine copulas are a special class of copulas based on conditioning ideas first proposed in Joe (1996) and later more developed and organized by Bedford & Cooke (2001). This approach allows any d -dimensional copula and its density to be expressed by $\frac{d(d-1)}{2}$ bivariate copulas and their densities. Moreover, the expression can be represented by an undirected graph structure (Bedford & Cooke, 2002), i.e., *regular vine (R-vine)*. A d -dimensional R-vine consists of $d - 1$ nested trees, each tree T_m has a node set V_m , and an edge set E_m for $m = 1, \dots, d - 1$. The edges in tree level m are the nodes in tree level $m + 1$, and a pair of nodes in tree T_{m+1} are allowed to be connected if they have a common node in tree T_m . A formal definition of Bedford & Cooke (2002) is that a structure $\mathcal{V} = (T_1, \dots, T_{d-1})$ is a regular vine on d elements if it meets the following conditions:

1. T_1 is a tree with node set $V_1 = \{1, \dots, d\}$ and edge set E_1 .
2. T_m is a tree with node set $V_m = E_{m-1}$ for $m = 2, \dots, d - 1$.
3. (*Proximity*) If an edge connects two nodes in T_{m+1} , their associated edges in T_m must have a shared node in T_m .

The structure $\mathcal{V} = (T_1, \dots, T_{d-1})$ is also called a *vine tree structure*, and truncating a vine after the first tree is equivalent to a Markov tree model (Brechmann et al., 2012). Thus, vines are the extending Markov trees in the sense that they allow conditional dependencies. For instance, selecting the parameters of the edges in the first tree level as correlations and the parameters of the edges in the next tree levels as partial correlations, where the partial correlations are conditioned on $m - 1$ variables in tree level m , in a vine can represent a multivariate Gaussian distribution when margins follow a univariate normal distribution.

Following the notation in Chapter 5 of Czado (2019), Figure 2 shows a 3-dimensional vine. The vine tree structure \mathcal{V} has two tree levels T_1 and T_2 . The first tree level T_1 consists of the node set $V_1 = \{1, 2, 3\}$ and the edge set $E_1 = \{\{1, 3\}, \{2, 3\}\}$. In the second tree level, the node set is $V_2 = E_1$, and the edge set is $E_2 = \{\{1, 2; 3\}\}$. The two nodes in T_2 are joined since they share the common node 3 in T_1 .

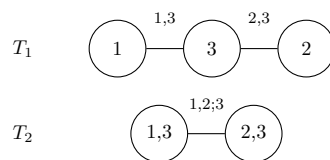


Figure 2: Example of a 3-dimensional regular vine.

To have a vine copula or *pair copula construction*, each edge in a vine tree structure is associated with a bivariate copula. For example, when the bivariate copulas $C_{1,3}$, $C_{2,3}$ are associated with E_1 , and the bivariate copula $C_{1,3;2}$ belongs to E_2 in the vine tree structure in Figure 2, a vine copula model is formed. Assume

each bivariate copula $C_{1,3}, C_{2,3}, C_{1,3;2}$ is parametric with the corresponding parameters $\boldsymbol{\theta}_{1,3}, \boldsymbol{\theta}_{2,3}, \boldsymbol{\theta}_{1,3;2}$ and admits the corresponding density $c_{1,3}, c_{2,3}, c_{1,3;2}$. Then we can write the density of this vine copula model for $\mathbf{U} = (U_1, U_2, U_3)^\top \in [0, 1]^3$ at $\mathbf{u} = (u_1, u_2, u_3)^\top$ as follows:

Example 2.1. *The density of a vine copula model corresponding to the vine tree structure in Figure 2*

$$g(u_1, u_2, u_3; \boldsymbol{\theta}) = c_{1,3}(u_1, u_3; \boldsymbol{\theta}_{1,3}) \cdot c_{2,3}(u_2, u_3; \boldsymbol{\theta}_{2,3}) \cdot c_{1,2;3}(G_{1|3}(u_1|u_3; \boldsymbol{\theta}_{1,3}), G_{2|3}(u_2|u_3; \boldsymbol{\theta}_{2,3}); u_3, \boldsymbol{\theta}_{1,2;3}), \quad (1)$$

where $\boldsymbol{\theta} = (\boldsymbol{\theta}_{1,3}, \boldsymbol{\theta}_{2,3}, \boldsymbol{\theta}_{1,2;3})^\top$ contains all pair copula parameters, and $G_{1|3}$ ($G_{2|3}$) is the conditional distribution of the random variable $U_1|U_3 = u_3$ ($U_2|U_3 = u_3$).

Vine copulas are flexible and powerful by using bivariate building blocks (pair copulas). Moreover, Sklar's Theorem (Sklar, 1959) states another flexibility of copulas: the density of a d -dimensional distribution can be decomposed into the product of its univariate marginal densities and the associated copula density. In the remainder, assume all random variables to be absolutely continuous. Then for a d -dimensional random vector $\mathbf{X} = (X_1, \dots, X_d)^\top \in \mathbb{R}^d$ following a joint distribution F with the univariate marginal distributions F_1, \dots, F_d and densities f_1, \dots, f_d , and a copula density c of the random vector $\mathbf{F} = (F_1(X_1), \dots, F_d(X_D))^\top \in [0, 1]^d$, the d dimensional joint density g can be written as

$$g(\mathbf{x}) = c(F_1(x_1), \dots, F_d(x_d)) \cdot f_1(x_1) \cdots f_d(x_d), \quad \mathbf{x} \in \mathbb{R}^d. \quad (2)$$

The vine copula model in Example 2.1 can formulate a 3-dimensional joint density g by Sklar's Theorem. Let F_1, F_2, F_3 denote parametric, univariate marginal distributions with the corresponding parameters $\gamma_1, \gamma_2, \gamma_3$, and f_1, f_2, f_3 indicate their densities.

Example 2.2. *The 3-dimensional joint density with the vine copula model of Example 2.1 is given by*

$$g(x_1, x_2, x_3; \boldsymbol{\psi}) = c_{1,3}(F_1(x_1; \gamma_1), F_3(x_3; \gamma_3); \boldsymbol{\theta}_{1,3}) \cdot c_{2,3}(F_2(x_2; \gamma_2), F_3(x_3; \gamma_3); \boldsymbol{\theta}_{2,3}) \cdot c_{1,2;3}(F_{1|3}(x_1|x_3; \gamma_1, \gamma_3, \boldsymbol{\theta}_{1,3}), F_{2|3}(x_2|x_3; \gamma_2, \gamma_3, \boldsymbol{\theta}_{2,3}); x_3, \boldsymbol{\theta}_{1,2;3}) \cdot f_1(x_1; \gamma_1) \cdot f_2(x_2; \gamma_2) \cdot f_3(x_3; \gamma_3), \quad (3)$$

where the vector $\boldsymbol{\psi}$ contains the marginal and pair copula parameters, $c_{1,2;3}(F_{1|3}(x_1|x_3), F_{2|3}(x_2|x_3); x_3)$ is the joint (copula) density corresponding to the random vector $(F_{1|3}(X_1|X_3), F_{2|3}(X_2|X_3))^\top$ given $X_3 = x_3$.

In Example 2.2, it is assumed that all marginal distributions are parametric, which we assume in the following, and estimate the margins accordingly. Thus, we follow the *inference for margins* (IFM) approach (Joe & Xu, 1996). Observe that the copula density $c_{1,2;3}$ depends on the specific value u_3 of the conditioning variable U_3 in Example 2.1 and the specific value x_3 of the conditioning variable X_3 in Example 2.2. However, we will ignore this dependence to reduce model complexity, i.e., make the *simplifying assumption*. Under the

simplifying assumption, the copula density $c_{1,2,3}$ does not have any conditional dependence on the specific value of u_3 or x_3 and is a 2-dimensional copula density. Nevertheless, it still depends on the conditioning value through its arguments. For more details, we refer to [Stöber et al. \(2013\)](#).

Example 2.3. *The 3-dimensional joint density g of Example 2.2 under the simplifying assumption is*

$$\begin{aligned} g(x_1, x_2, x_3; \boldsymbol{\psi}) = & c_{1,3}(F_1(x_1; \boldsymbol{\gamma}_1), F_3(x_3; \boldsymbol{\gamma}_3); \boldsymbol{\theta}_{1,3}) \cdot c_{2,3}(F_2(x_2; \boldsymbol{\gamma}_2), F_3(x_3; \boldsymbol{\gamma}_3); \boldsymbol{\theta}_{2,3}) \\ & \cdot c_{1,2,3}(F_{1|3}(x_1|x_3; \boldsymbol{\gamma}_1, \boldsymbol{\gamma}_3, \boldsymbol{\theta}_{1,3}), F_{2|3}(x_2|x_3; \boldsymbol{\gamma}_2, \boldsymbol{\gamma}_3, \boldsymbol{\theta}_{2,3}); \boldsymbol{\theta}_{1,2,3}) \\ & \cdot f_1(x_1; \boldsymbol{\gamma}_1) \cdot f_2(x_2; \boldsymbol{\gamma}_2) \cdot f_3(x_3; \boldsymbol{\gamma}_3). \end{aligned} \quad (4)$$

For a general dimension d , a d -dimensional joint density is similarly constructed using d marginal densities and $\frac{d \cdot (d-1)}{2}$ associated pair-copula densities. Let $c_{e_a, e_b; D_e}$ be a parametric pair copula density associated with an edge e in vine tree structure \mathcal{V} and $\boldsymbol{\theta}_{e_a, e_b; D_e}$ be its parameters ($e \in E_m$, for $m = 1, \dots, d-1$). Let f_p denote a parametric, univariate marginal density with the parameters $\boldsymbol{\gamma}_p$ for $p = 1, \dots, d$. Then a d -dimensional joint density g under the simplifying assumption can be constructed as follows:

$$\begin{aligned} g(\boldsymbol{x}; \boldsymbol{\psi}) = & \prod_{m=1}^{d-1} \prod_{e \in E_m} c_{e_a, e_b; D_e}(F_{e_a|D_e}(x_{e_a}|\boldsymbol{x}_{D_e}; \boldsymbol{\gamma}_{e_a|D_e}, \boldsymbol{\theta}_{e_a|D_e}), F_{e_b|D_e}(x_{e_b}|\boldsymbol{x}_{D_e}; \boldsymbol{\gamma}_{e_b|D_e}, \boldsymbol{\theta}_{e_b|D_e}); \boldsymbol{\theta}_{e_a, e_b; D_e}) \\ & \cdot \prod_{p=1}^d f_p(x_p; \boldsymbol{\gamma}_p), \end{aligned} \quad (5)$$

where $\boldsymbol{x}_{D_e} = (x_z)_{z \in D_e}$ is a subvector of $\boldsymbol{x} = (x_1, \dots, x_d)^\top \in \mathbb{R}^d$, the parameter vector $\boldsymbol{\psi}$ contains the marginal and pair copula parameters, $F_{e_a|D_e}$ is the conditional distribution function of the random variable $X_{e_a} | \boldsymbol{X}_{D_e} = \boldsymbol{x}_{D_e}$. It can be calculated recursively ([Joe, 1996](#)). The marginal $\boldsymbol{\gamma}_{e_a|D_e}$ and pair copula $\boldsymbol{\theta}_{e_a|D_e}$ parameters are used to determine $F_{e_a|D_e}$. The set D_e is called the *conditioning set*, and the indices e_a, e_b form the *conditioned set*. D_e has $m-1$ elements in tree level m ; therefore, it is empty in the first tree.

3. Vine copula mixture models

We now introduce a vine copula mixture model and describe approaches for model selection and parameter estimation problems in the following subsections. The model is fully parametric, i.e., it works with parametric pair copulas and univariate marginal distributions.

3.1. Model formulation

Suppose the data consists of n observations, where an observation $\boldsymbol{x}_i = (x_{i,1}, \dots, x_{i,d})^\top$ is an independent realization of a d -dimensional random vector $\boldsymbol{X} = (X_1, \dots, X_d)^\top$ for $i = 1, \dots, n$. Assume that a mixture of k components ($k \in \mathbb{R}^+$) generates the data, and the density g_j of the j th component for $j = 1, \dots, k$ can be stated by Sklar's Theorem as given in Equation (5). Assume that, additionally, the j th component has

a mixture weight π_j with $\pi_j \in (0, 1)$ for $j = 1, \dots, k$ and $\sum_j^k \pi_j = 1$. Then the density of the vine copula mixture model for $\mathbf{X} = (X_1, \dots, X_d)^\top$ at $\mathbf{x} = (x_1, \dots, x_d)^\top$ can be written as:

$$g(\mathbf{x}; \boldsymbol{\eta}) = \sum_{j=1}^k \pi_j \cdot g_j(\mathbf{x}; \boldsymbol{\psi}_j). \quad (6)$$

Here the vector $\boldsymbol{\psi}_j$ contains the marginal and pair copula parameters of the j th component, $\boldsymbol{\eta}$ denotes all model parameters, i.e., $\boldsymbol{\eta} = (\boldsymbol{\eta}_1, \dots, \boldsymbol{\eta}_k)^\top$ and $\boldsymbol{\eta}_j = (\pi_j, \boldsymbol{\psi}_j)^\top$ for $j = 1, \dots, k$.

Example 3.1. *Vine copula mixture model formulation in three dimensions with two components*

Assume data, where an observation $\mathbf{x}_i = (x_{i,1}, x_{i,2}, x_{i,3})^\top$ for $i = 1, \dots, n$ is given, and there are two components generating the data with the mixture weights $\pi_1 > 0$ and $\pi_2 > 0$ ($\pi_1 + \pi_2 = 1$). An observation of the first and second component is an independent realization of a 3-dimensional random vector $\mathbf{X}_{(1)} = (X_{1(1)}, X_{2(1)}, X_{3(1)})^\top$ and $\mathbf{X}_{(2)} = (X_{1(2)}, X_{2(2)}, X_{3(2)})^\top$, respectively. Figure 3 shows the vine copula model of each component. $T_{(1)1}$ and $T_{(2)1}$ represent the first tree, whereas $T_{(1)2}$ and $T_{(2)2}$ refer to the second tree of the first and second component. The edge sets of the first component are $E_{(1)1} = \{\{1, 2\}, \{2, 3\}\}$, $E_{(1)2} = \{1, 3; 2\}$ and that of the second component are $E_{(2)1} = \{\{1, 2\}, \{1, 3\}\}$, $E_{(2)2} = \{2, 3; 1\}$, respectively.

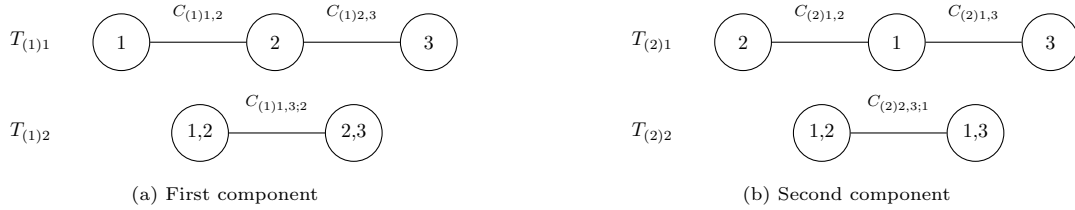


Figure 3: Vine copula model of two components.

The pair copula families and marginal distributions of both components are parametric. $C_{(1)1,2}$, $C_{(1)1,2,3}$, $C_{(1)1,3;2}$ denote pair copula families of the first component associated with the edges in $E_{(1)1}$ and $E_{(1)2}$, while $\boldsymbol{\theta}_{(1)1,2}$, $\boldsymbol{\theta}_{(1)1,2,3}$, $\boldsymbol{\theta}_{(1)1,3;2}$ show the corresponding parameters. For the second component, we use notations $C_{(2)1,2}$, $C_{(2)1,3}$, $C_{(2)2,3;1}$ for pair copula families associated with the edges in $E_{(2)1}$ and $E_{(2)2}$, and $\boldsymbol{\theta}_{(2)1,2}$, $\boldsymbol{\theta}_{(2)1,3}$, $\boldsymbol{\theta}_{(2)2,3;1}$ refer to the corresponding parameters. A copula density is denoted by the small c letter. $F_{1(1/2)}$, $F_{2(1/2)}$, $F_{3(1/2)}$ refer to the marginal distributions of the random variables $X_{1(1/2)}$, $X_{2(1/2)}$, $X_{3(1/2)}$ with the corresponding parameters $\gamma_{1(1/2)}$, $\gamma_{2(1/2)}$, $\gamma_{3(1/2)}$ for the first/second component. The small f letter denotes a marginal density. We can write the **density of the first component** at $\mathbf{x} = (x_1, x_2, x_3)^\top$:

$$\begin{aligned} g_1(\mathbf{x}; \boldsymbol{\psi}_1) = & c_{(1)1,2}(F_{1(1)}(x_1; \gamma_{1(1)}), F_{2(1)}(x_2; \gamma_{2(1)}); \boldsymbol{\theta}_{(1)1,2}) \cdot c_{(1)2,3}(F_{2(1)}(x_2; \gamma_{2(1)}), F_{3(1)}(x_3; \gamma_{3(1)}); \boldsymbol{\theta}_{(1)2,3}) \\ & \cdot c_{(1)1,3;2}(F_{(1)1|2}(x_1|x_2; \gamma_{1(1)}, \gamma_{2(1)}, \boldsymbol{\theta}_{(1)1,2}), F_{(1)3|2}(x_3|x_2; \gamma_{3(1)}, \gamma_{2(1)}, \boldsymbol{\theta}_{(1)2,3}); \boldsymbol{\theta}_{(1)1,3;2}) \\ & \cdot f_{1(1)}(x_1; \gamma_{1(1)}) \cdot f_{2(1)}(x_2; \gamma_{2(1)}) \cdot f_{3(1)}(x_3; \gamma_{3(1)}), \end{aligned} \quad (7)$$

where the pair copula parameters used to determine the conditional distribution functions $F_{(1)1|2}$ and $F_{(1)3|2}$ are given by $\boldsymbol{\theta}_{(1)1|2} = \boldsymbol{\theta}_{(1)1,2}$ and $\boldsymbol{\theta}_{(1)3|2} = \boldsymbol{\theta}_{(1)2,3}$, respectively. The marginal parameters needed for the same calculation are denoted by $\boldsymbol{\gamma}_{(1)1|2} = (\boldsymbol{\gamma}_{1(1)}, \boldsymbol{\gamma}_{2(1)})^\top$ and $\boldsymbol{\gamma}_{(1)3|2} = (\boldsymbol{\gamma}_{2(1)}, \boldsymbol{\gamma}_{3(1)})^\top$. We show the marginal and pair copula parameters of the first component by $\boldsymbol{\psi}_1 = (\boldsymbol{\gamma}_1, \boldsymbol{\theta}_1)^\top$, where $\boldsymbol{\gamma}_1 = (\boldsymbol{\gamma}_{1(1)}, \boldsymbol{\gamma}_{2(1)}, \boldsymbol{\gamma}_{3(1)})^\top$ and $\boldsymbol{\theta}_1 = (\boldsymbol{\theta}_{(1)1,2}, \boldsymbol{\theta}_{(1)2,3}, \boldsymbol{\theta}_{(1)1,3;2})^\top$. As in the first component, we can define the parameters and write the **second component density** at $\mathbf{x} = (x_1, x_2, x_3)^\top$:

$$\begin{aligned} g_2(\mathbf{x}; \boldsymbol{\psi}_2) &= c_{(2)1,2}(F_{1(2)}(x_1; \boldsymbol{\gamma}_{1(2)}), F_{2(2)}(x_2; \boldsymbol{\gamma}_{2(2)}); \boldsymbol{\theta}_{(2)1,2}) \cdot c_{(2)1,3}(F_{1(2)}(x_1; \boldsymbol{\gamma}_{1(2)}), F_{3(2)}(x_3; \boldsymbol{\gamma}_{3(2)}); \boldsymbol{\theta}_{(2)1,3}) \\ &\quad \cdot c_{(2)2,3;1}(F_{(2)2|1}(x_2|x_1; \boldsymbol{\gamma}_{2(2)}, \boldsymbol{\gamma}_{1(2)}, \boldsymbol{\theta}_{(2)1,2}), F_{(2)3|1}(x_3|x_1; \boldsymbol{\gamma}_{3(2)}, \boldsymbol{\gamma}_{1(2)}, \boldsymbol{\theta}_{(2)1,3}); \boldsymbol{\theta}_{(2)2,3;1}) \\ &\quad \cdot f_{1(2)}(x_1; \boldsymbol{\gamma}_{1(2)}) \cdot f_{2(2)}(x_2; \boldsymbol{\gamma}_{2(2)}) \cdot f_{3(2)}(x_3; \boldsymbol{\gamma}_{3(2)}), \end{aligned} \tag{8}$$

As a result, the **vine copula mixture model density** at $\mathbf{x} = (x_1, x_2, x_3)^\top$ is given by

$$g(\mathbf{x}; \boldsymbol{\eta}) = \pi_1 g_1(\mathbf{x}; \boldsymbol{\psi}_1) + \pi_2 g_2(\mathbf{x}; \boldsymbol{\psi}_2), \tag{9}$$

where $\boldsymbol{\eta}_1 = (\pi_1, \boldsymbol{\psi}_1)^\top$ and $\boldsymbol{\eta}_2 = (\pi_2, \boldsymbol{\psi}_2)^\top$ indicate the model parameters of the first and second component. All model parameters are given by $\boldsymbol{\eta} = (\boldsymbol{\eta}_1, \boldsymbol{\eta}_2)^\top$.

3.2. Model selection

Vine copula mixture models inherit the problem of estimating the total number of components k hidden in the data from the finite mixture models. Moreover, due to its formulation in Equations (5) and (6), the vine tree structure \mathcal{V}_j , pair copula families $\mathcal{B}_j(\mathcal{V}_j)$, and marginal distributions $\mathcal{F}_j = \{F_{1(j)}, \dots, F_{d(j)}\}$ of the j th component need to be chosen for $j = 1, \dots, k$. Accordingly, pair copula parameters $\boldsymbol{\theta}_j(\mathcal{B}_j(\mathcal{V}_j))$ and marginal parameters $\boldsymbol{\gamma}_j(\mathcal{F}_j)$ should be estimated for $j = 1, \dots, k$. To simplify, we will assume that the total number of components generating the data is known. If a priori information about k does not exist, methods that estimate it from the data need to be developed for vine copula mixture models. However, it is currently not the focus of our work. Instead, we will explain the approaches to the remaining model selection problems in the following and discuss the parameter estimation in Section 3.3.

Assume an observation $\mathbf{x}_i = (x_{i,1}, \dots, x_{i,d})^\top$ is assigned to a component for $i = 1, \dots, n$. We will learn model components with the assignment, use the vine copula mixture models for clustering applications, and explain assignment approaches in Algorithm 1 in Section 4. We will show the promising results of this approach in Sections 5 and 6 and discuss a modification, when it is hard to learn model components, e.g., components have non-negligible overlaps, in Section 5.3.

Assume the total number of observations assigned to the j th component is n_j , and the observations belonging to the j th component are given by $\mathbf{x}_{(j)i_j} = (x_{(j)i_j,1}, \dots, x_{(j)i_j,d})^\top$ for $i_j = 1, \dots, n_j$ and $j = 1, \dots, k$. It holds that $\sum_{j=1}^k n_j = n$ and $\bigcup_{\forall(j,i_j)} \mathbf{x}_{(j)i_j} = \bigcup_{\forall i} \mathbf{x}_i$. We denote the p th variable in the j th component by

$\mathbf{x}_{p(j)} = (x_{(j)1,p}, \dots, x_{(j)n_j,p})^\top$ for $p = 1, \dots, d$ and $j = 1, \dots, k$. With the given assignment, we first select the marginal distributions of each cluster. Such a candidate set could be prespecified or chosen by a data analysis such as a histogram and quantile-quantile (QQ) plot. Then the marginal distribution family $F_{p(j)}$ for the variable $\mathbf{x}_{p(j)}$ will be determined using a model selection criteria. More precisely:

- **Marginal distribution selection** \mathcal{F}_j : For $p = 1, \dots, d$ and $j = 1, \dots, k$, the log-likelihood of the marginal distribution $F_{p(j)}$ with the density $f_{p(j)}$ and parameters $\gamma_{p(j)}$ on the variable $\mathbf{x}_{p(j)}$ is

$$\ell(\gamma_{p(j)}) = \sum_{i=1}^{n_j} \log (f_{p(j)}(x_{(j)i,p}; \gamma_{p(j)})) \quad \text{for } p = 1, \dots, d \quad \text{and } j = 1, \dots, k. \quad (10)$$

The BIC, a commonly used model selection criteria, is given by

$$BIC(\gamma_{p(j)}) = -2 \cdot \ell(\gamma_{p(j)}) + |\gamma_{p(j)}| \cdot \log (n_j) \quad \text{for } p = 1, \dots, d \quad \text{and } j = 1, \dots, k, \quad (11)$$

where $|\gamma_{p(j)}|$ refers to the number of marginal parameters in $F_{p(j)}$, and n_j denotes the total number of observations in $\mathbf{x}_{p(j)}$. For each candidate for the marginal distribution on the variable $\mathbf{x}_{p(j)}$, first, the parameters that maximize the log-likelihood $\ell(\gamma_{p(j)})$ are estimated, then the marginal distribution family with the lowest BIC is selected.

Since the joint density can be decomposed into univariate marginal densities and a vine copula density by Sklar's Theorem, we now estimate the u-data for a vine copula model by applying the probability integral transformation using the estimated margins $\hat{F}_{p(j)}$ for each cluster: $\hat{\mathbf{u}}_{p(j)} = \hat{F}_{p(j)}(\mathbf{x}_{p(j)}; \hat{\gamma}_{p(j)})$ and set $\hat{\mathbf{u}}_{p(j)} = (\hat{u}_{(j)1,p}, \dots, \hat{u}_{(j)n_j,p})^\top$. After obtaining the u-data of the j th component, the best selection of \mathcal{V}_j would be the true structure selection, but the total number of vine tree structures on d variables is $\frac{d!}{2} \cdot 2^{\binom{d-2}{2}}$ (Morales-Nápoles, 2010). If d is small, it is possible to enumerate all possible structures. However, it is usually not a feasible approach, even with small dimensions, as one also needs to select pair copula families for each scenario. Therefore, a greedy algorithm proposed for the vine tree and pair copula family selection might be used for each component. For instance, we use the greedy algorithm of Dißmann et al. (2013) in Algorithm 1. Briefly, it works as follows:

- **Vine tree structure selection** \mathcal{V}_j : For $j = 1, \dots, k$, it proceeds sequentially tree by tree, starting from tree one, and finds the maximum spanning tree at each tree among all edges allowed by proximity. Edge weight is the absolute empirical Kendall's τ value between the pair of nodes forming the edge.
- **Pair copula family selection** $\mathcal{B}_j(\mathcal{V}_j)$: For $j = 1, \dots, k$, after learning the vine tree structure, pair copula families of the given structure are also estimated sequentially tree by tree. For a parametric pair copula $C_{(j)e_a, e_b; D_e}$ associated with an edge e in \mathcal{V}_j with the density $c_{(j)e_a, e_b; D_e}$ and parameters $\theta_{(j)e_a, e_b; D_e}$, one first estimates the parameters that maximize the log-likelihood $\ell(\theta_{(j)e_a, e_b; D_e})$. Later

the copula family with the lowest Akaike Information Criterion (AIC) (Akaike, 1998) is chosen:

$$AIC(\boldsymbol{\theta}_{(j)e_a, e_b; D_e}) = -2 \cdot \ell(\boldsymbol{\theta}_{(j)e_a, e_b; D_e}) + 2 \cdot |\boldsymbol{\theta}_{(j)e_a, e_b; D_e}| \quad \text{for } j = 1, \dots, k \quad \text{and } e \in \mathcal{V}_j, \quad (12)$$

where $|\boldsymbol{\theta}_{(j)e_a, e_b; D_e}|$ denotes the number of copula parameters in $c_{(j)e_a, e_b; D_e}$. One does not need an alternative selection criterion like the BIC to induce model sparsity for the pair copula family selection when the fitted pair copula families have one or two parameters as later proposed in Algorithm 1.

3.3. Parameter estimation

Given that the marginal distributions, vine tree structure, and associated pair copula families of each component are selected and known, a first task in the vine copula mixture model is to estimate the model parameters $\boldsymbol{\eta}$ in Equation (6). The optimal parameter estimates would be the values that maximize the log-likelihood of the given data defined in Equation (13):

$$\ell(\boldsymbol{\eta}) = \log \prod_{i=1}^n g(\mathbf{x}_i; \boldsymbol{\psi}) = \log \prod_{i=1}^n \sum_{j=1}^k \pi_j \cdot g_j(\mathbf{x}_i; \boldsymbol{\psi}_j). \quad (13)$$

Nevertheless, the true assignment of the observations to each component is unknown, and the parameter estimates would change depending on the component to which an observation belongs. As a solution to this problem, the expectation-maximization (EM) algorithm (Dempster et al., 1977) views the observations $\mathbf{x}_i = (x_{i,1}, \dots, x_{i,d})^\top$ as incomplete and introduces latent variables $\mathbf{z}_i = (z_{i,1}, \dots, z_{i,k})^\top$, where each element $z_{i,j}$ is a binary variable defined as

$$z_{i,j} = \begin{cases} 1, & \text{if } \mathbf{x}_i \text{ belongs to the } j\text{th component,} \\ 0, & \text{otherwise,} \end{cases} \quad (14)$$

and $\sum_{j=1}^k z_{i,j} = 1$. The random vector \mathbf{Z}_i corresponding to \mathbf{z}_i follows a multinomial distribution with one trial and probabilities π_1, \dots, π_k , that is, $\mathbf{Z}_i \sim \text{Mult}(1, \boldsymbol{\pi} = (\pi_1, \dots, \pi_k))$. Then we can write the *complete data log-likelihood* $\ell_c(\boldsymbol{\eta}; \mathbf{z}, \mathbf{x})$ of the complete data $\mathbf{y}_i = (\mathbf{x}_i, \mathbf{z}_i)^\top$ from Equation (6) as:

$$\ell_c(\boldsymbol{\eta}; \mathbf{z}, \mathbf{x}) = \log \prod_{i=1}^n \prod_{j=1}^k [\pi_j \cdot g_j(\mathbf{x}_i; \boldsymbol{\psi}_j)]^{z_{i,j}} = \sum_{i=1}^n \sum_{j=1}^k z_{i,j} \cdot \log \pi_j + \sum_{i=1}^n \sum_{j=1}^k z_{i,j} \cdot \log g_j(\mathbf{x}_i; \boldsymbol{\psi}_j), \quad (15)$$

where $g_j(\mathbf{x}_i; \boldsymbol{\psi}_j)$ is given in Equation (5). Hence, we can write:

$$\begin{aligned} \ell_c(\boldsymbol{\eta}; \mathbf{z}, \mathbf{x}) &= \sum_{i=1}^n \sum_{j=1}^k [z_{i,j} \cdot \log \pi_j] + \sum_{i=1}^n \sum_{j=1}^k \sum_{p=1}^d [z_{i,j} \cdot \log f_{p(j)}(x_{i,p}; \boldsymbol{\gamma}_{p(j)})] \\ &+ \sum_{i=1}^n \sum_{j=1}^k \sum_{m=1}^{d-1} \sum_{e \in E_{(j)m}} [z_{i,j} \cdot \log c_{(j)e_a, e_b; D_e}(F_{(j)e_a|D_e}(x_{i,e_a} | \mathbf{x}_{i,D_e}; \boldsymbol{\gamma}_{(j)e_a|D_e}, \boldsymbol{\theta}_{(j)e_a|D_e}), \\ &F_{(j)e_b|D_e}(x_{i,e_b} | \mathbf{x}_{i,D_e}; \boldsymbol{\gamma}_{(j)e_b|D_e}, \boldsymbol{\theta}_{(j)e_b|D_e}); \boldsymbol{\theta}_{(j)e_a, e_b; D_e})]. \end{aligned} \quad (16)$$

Note that we use $\boldsymbol{\theta}_j$ for the pair copula parameters instead of $\boldsymbol{\theta}_j(\mathcal{B}_j(\mathcal{V}_j))$ and $\boldsymbol{\gamma}_j$ for the marginal parameters instead of $\boldsymbol{\gamma}_j(\mathcal{F}_j)$ to simplify notation.

The EM algorithm alternates the E and M steps, increasing the data log-likelihood at each iteration (Dempster et al., 1977). The E-step requires calculating the conditional expectation of the complete-data log likelihood, given the observed data and current parameter estimates. The M-step maximizes the expected complete data log-likelihood from the E-step over all parameters. We need to estimate marginal parameters $\boldsymbol{\gamma}_j$, pair copula parameters $\boldsymbol{\theta}_j$, and mixture weight π_j of the j th component. Since their joint estimation is not tractable and efficient, we use the expectation conditional maximum (ECM) algorithm (Meng & Rubin, 1993). Here, the M-step in the EM is replaced by three lower dimensional maximization problems called CM-steps. The vine tree structure, associated pair copula families and marginal distributions remain fixed at the initial choice for each component in the ECM iterations. Then the $(t + 1)$ th iteration steps are

1. **E-step (Posterior probabilities)**: Calculate the posterior probability that an observation \mathbf{x}_i belongs to the j th component given the current values of the model parameters $\pi_j^{(t)}$ and $\boldsymbol{\psi}_j^{(t)} = (\boldsymbol{\gamma}_j^{(t)}, \boldsymbol{\theta}_j^{(t)})^\top$:

$$r_{i,j}^{(t+1)} = \frac{\pi_j^{(t)} g_j(\mathbf{x}_i; \boldsymbol{\psi}_j^{(t)})}{\sum_{j'=1}^k \pi_{j'}^{(t)} g_{j'}(\mathbf{x}_i; \boldsymbol{\psi}_{j'}^{(t)})} \quad \text{for } i = 1, \dots, n \quad \text{and } j = 1, \dots, k. \quad (17)$$

2. **CM-step 1 (Mixture weights)**: Maximize $\ell_c(\boldsymbol{\eta}; \mathbf{z}, \mathbf{x})$ over π_j given the updated posterior probabilities $r_{i,j}^{(t+1)}$:

$$\pi_j^{(t+1)} = \arg \max_{\pi_j} \sum_{i=1}^n r_{i,j}^{(t+1)} \cdot \log \pi_j \quad \text{for } j = 1, \dots, k. \quad (18)$$

A closed form solution exists and is given by

$$\pi_j^{(t+1)} = \frac{\sum_{i=1}^n r_{i,j}^{(t+1)}}{n} \quad \text{for } j = 1, \dots, k. \quad (19)$$

3. **CM-step 2 (Marginal parameters)**: Optimal marginal parameter estimates $\boldsymbol{\gamma}_j^*$ of the j th component would maximize $\ell_c(\boldsymbol{\eta}; \mathbf{z}, \mathbf{x})$ over $\boldsymbol{\gamma}_j$ given the current values of the pair copula parameters $\boldsymbol{\theta}_j^{(t)}$ and updated posterior probabilities $r_{i,j}^{(t+1)}$:

$$\boldsymbol{\gamma}_j^* = \arg \max_{\boldsymbol{\gamma}_j} \sum_{i=1}^n r_{i,j}^{(t+1)} \cdot \log g_j(\mathbf{x}_i; \boldsymbol{\gamma}_j, \boldsymbol{\theta}_j^{(t)}) \quad \text{for } j = 1, \dots, k. \quad (20)$$

However, since a closed form solution does not exist, we numerically maximize $\ell_c(\boldsymbol{\eta}; \mathbf{z}, \mathbf{x})$ over $\boldsymbol{\gamma}_j$

$$\max_{\boldsymbol{\gamma}_j} \sum_{i=1}^n r_{i,j}^{(t+1)} \cdot \log g_j(\mathbf{x}_i; \boldsymbol{\gamma}_j, \boldsymbol{\theta}_j^{(t)}) \quad \text{for } j = 1, \dots, k \quad (21)$$

to find the updated values of the marginal parameters $\boldsymbol{\gamma}_j^{(t+1)}$.

4. **CM-step 3 (Pair copula parameters)**: Again, a closed form solution that maximizes $\ell_c(\boldsymbol{\eta}; \mathbf{z}, \mathbf{x})$ over $\boldsymbol{\theta}_j$ given the current values of the marginal parameters $\boldsymbol{\gamma}_j^{(t+1)}$ and updated posterior probabilities $r_{i,j}^{(t+1)}$ does not exist. Hence, we numerically maximize $\ell_c(\boldsymbol{\eta}; \mathbf{z}, \mathbf{x})$ over $\boldsymbol{\theta}_j$

$$\max_{\boldsymbol{\theta}_j} \sum_{i=1}^n r_{i,j}^{(t+1)} \cdot \log g_j(\mathbf{x}_i; \boldsymbol{\gamma}_j^{(t+1)}, \boldsymbol{\theta}_j) \quad \text{for } j = 1, \dots, k \quad (22)$$

to find the updated values of the pair copula parameters $\boldsymbol{\theta}_j^{(t+1)}$. In the case of a d -dimensional vine copula with parametric pair copulas, the total number of pair copula parameters to be estimated grows quadratically in dimension d . However, truncating a vine tree structure at tree level 1, i.e., obtaining a Markov tree, reduces the total number of parameter estimates linear in dimension d , one of the main motivations for the third step's formulation with Markov trees in Algorithm 1.

Starting values and stopping condition

For the ECM algorithm, we require initial parameters $\boldsymbol{\eta}_j^{(0)}$ of the j th component for $j = 1, \dots, k$. Since the marginal distributions, vine tree structure, and associated pair copula families of each component stay fixed in the ECM iterations, we, additionally, need to select them. One method is to select an initial partition in advance. A more general alternative, given in Algorithm 1, uses quick clustering algorithms with possible weights of observations $\mathbf{x}_i = (x_{i,1}, \dots, x_{i,d})^\top$ for $i = 1, \dots, n$ in different components to have a starting partition. Assume that the total number of observations assigned to the j th component at the 0th iteration is $n_j^{(0)}$, and the observations belonging to the j th component at the 0th iteration are given by $\mathbf{x}_{(j)i_j}^{(0)} = (x_{(j)i_j,1}^{(0)}, \dots, x_{(j)i_j,d}^{(0)})^\top$ for $i_j = 1, \dots, n_j^{(0)}$ and $j = 1, \dots, k$. It holds that $\sum_{j=1}^k n_j^{(0)} = n$ and $\bigcup_{\forall(j,i_j)} \mathbf{x}_{(j)i_j}^{(0)} = \bigcup_{\forall i} \mathbf{x}_i$. After specifying an initial set for parametric marginal distributions, vine tree structures and associated parametric pair copula families, the starting values can be obtained as follows:

1. Initial marginal distributions $F_{p(j)}^{(0)}$ and marginal parameters $\boldsymbol{\gamma}_{p(j)}^{(0)}$: For $j = 1, \dots, k$ and $p = 1, \dots, d$, the marginal parameters maximize the log-likelihood of a variable $\mathbf{x}_{p(j)}^{(0)} = (x_{(j)1,p}^{(0)}, \dots, x_{(j)n_j^{(0)},p}^{(0)})^\top$ given in Equation (10), then the marginal distribution with the lowest BIC given in Equation (11) is chosen as described in Section 3.2.
2. Initial vine tree structure $\mathcal{V}_j^{(0)}$, pair copula families $\mathcal{V}_j^{(0)}(\mathcal{B}_j^{(0)})$ and its parameters $\boldsymbol{\theta}_{(j)}^{(0)}$: For $j = 1, \dots, k$ and $p = 1, \dots, d$, first, the cumulative distribution function of the chosen marginal distribution $F_{p(j)}^{(0)}$ with parameters $\boldsymbol{\gamma}_{p(j)}^{(0)}$ on the variable $\mathbf{x}_{p(j)}^{(0)}$ is fitted to obtain u-data of the j th component, $\mathbf{u}_{p(j)}^{(0)} = F_{p(j)}^{(0)}(\mathbf{x}_{p(j)}^{(0)}; \boldsymbol{\gamma}_{p(j)}^{(0)})$. The estimated u-data is then used to select a vine or Markov tree and the associated pair copula families with their parameters as discussed in Section 3.2.
3. Initial mixture weights $\pi_{(j)}^{(0)}$: For $j = 1, \dots, k$, they are proportional to the total number of observations belonging to the j th component and given by $\pi_{(j)}^{(0)} = \frac{n_j^{(0)}}{n}$.

The ECM is sensitive to the starting values, and a poor choice of them may result in convergence to a local maximum as an EM-type algorithm (Karlis & Xekalaki, 2003). However, our starting values optimize an associated model selection criterion based on the data log-likelihood. Even though there is no guarantee that the vine copula mixture model initialized by a fast clustering algorithm will select the correct model components, and its ECM iterations will converge to the global optimum, we show promising results of our current setup and discuss modifications with simulation studies in Section 5 and real data sets in Section 6.

A stopping criterion terminates the algorithm when the relative difference in the data log-likelihood between two successive iterations is less than the desired tolerance. We use the tolerance level (*tol*) 0.00001 in our simulation studies and real data analysis for clustering.

$$\frac{\ell(\boldsymbol{\eta}^{(t+1)}) - \ell(\boldsymbol{\eta}^{(t)})}{\ell(\boldsymbol{\eta}^{(t)})} < \textit{tol} \quad \text{for } t = 1, \dots, (s - 1). \quad (23)$$

4. Model-based clustering algorithm: VCMM

This section will formulate a model-based clustering algorithm (VCMM) with vine copula mixture models introduced in Section 3. We provide our pseudo-code in Algorithm 1 and give an overview flowchart in Appendix B. It consists of six primary building blocks and implements them in R (R Core Team, 2019).

The first step (initial clustering assignment via a fast clustering algorithm) partitions observations $\boldsymbol{x}_i = (x_{i,1}, \dots, x_{i,d})^\top$ for $i = 1, \dots, n$ into k components (clusters) using a quick clustering algorithm. Our analyses will mostly use the distance-based clustering, k-means (Hartigan & Wong, 1979) algorithm, with default specifications used in the package `stats`. Alternative clustering algorithms or partitions could be specified based on the analyzed data set. We will present an exemplary scenario in Section 5.3. For clustering algorithms, which are sensitive to the variables' scale, like k-means, we apply a standardization for each variable using the function `scale`. Since these algorithms might depend on the seed, we will present a real data analysis in Section 6.1 to guide choosing a good option.

As a second step, we select an initial VCMM model. The marginal distributions are determined among a candidate set of univariate parametric distributions by a model selection criteria. As discussed in Section 3.2, the parametric families in the candidate set could be chosen after initial graphical data analysis as given in the top left of Figure 1. In the paper, our candidate set for margins is normal, Student's t with degrees of freedom 3, logistic, log-normal, log-logistic, and gamma distribution. Thus, the algorithm allows also for a heavy-tailed marginal distribution. We can easily incorporate further marginal distributions into our algorithm. However, its current version can estimate the marginal distributions of the real data sets reasonably well, as shown in Section 6. We first truncate a vine tree structure at tree level one for the initial selection of vine copula models, thereby obtaining a Markov tree model. As discussed in Section 3.3, working with Markov trees allows us to decrease the optimization problem's size (CM-step 3) from quadratic to linear in dimension d , thereby reducing our computational effort. However, the performance of

using different truncation levels might be investigated in the future. A wide range of parametric pair copula families is applicable. Our algorithm’s pair copula families are parametric: Gaussian, t, Clayton, Gumbel, Frank, Joe, BB1, BB6, and BB8 copula. Since we apply their possible 90° , 180° , 270° rotations, the total number of pair copula families utilized is 27. Chapter 3 of [Czado \(2019\)](#) provides more details about them. For this part, we work with the package `VineCopula` and mainly its function `RVineStructureSelect` ([Nagler et al., 2019b](#)). The VCMM selects $d \cdot k$ marginal distributions, k Markov tree structures, and $(d-1) \cdot k$ pair copula families at this initial step.

The third step (parameter estimation via the ECM algorithm allowing for Markov (vine) tree structures) updates the VCMM parameters while keeping the marginal distributions, Markov tree structures, and pair copula families fixed until the stopping condition discussed in Section 3.3 holds. For each cluster, its mixture weight, pair copula parameters, and marginal parameters are updated per iteration. The total number of updated parameters per iteration is the sum of the total number of pair copula parameters, marginal parameters, and mixture weights over k clusters. Assume the ECM stops after s iterations. The total number of updated parameters up to this point is linear in dimension d , the total number of clusters k , and iterations s .

Next, we partition the observations into k clusters with the updated posterior probabilities as a temporary clustering assignment. An observation is a member of the cluster, where its posterior probability is highest.

The marginal distributions and dependence structure of the clusters can change due to the successive ECM steps. Moreover, dependencies can exist in higher tree levels, and accounting for those can improve model power. Thus, we perform a final model selection, and it is based on a full vine specification. The fifth step estimates the model components, including all possible vine tree levels and their parameters, with the fourth step’s clustering assignment. The VCMM chooses $d \cdot k$ marginal distributions, k vine tree structures, and $\frac{d \cdot (d-1)}{2} \cdot k$ pair copula families. The total number of updated parameters with this final step is linear in the total number of clusters k and iterations s , as in the third step, but is quadratic in dimension d due to the estimation of all possible vine tree levels. Using a full vine specification introduces additional parameter estimates; however, it increases model power as shown in Section 6.1.

The last step (final clustering assignment based on the full vine specification) assigns the observations to the clusters with the final model’s posterior probabilities.

Algorithm 1 Vine copula mixture models clustering: VCMM

- 1: **Input:** d -dimensional n observations to cluster $\mathbf{x}_i = (x_{i,1}, \dots, x_{i,d})^\top \in \mathbb{R}^d$ for $i = 1, \dots, n$ and total number of clusters k .
 - 2: **Output:** A clustering partition of the observations $\mathcal{C} = \{\mathcal{C}_1, \dots, \mathcal{C}_k\}$, estimated model components and parameters of the j th cluster defined in Section 3 $\hat{\mathcal{F}}_j, \hat{\gamma}_j, \hat{\mathcal{V}}_j, \hat{\mathcal{B}}_j(\hat{\mathcal{V}}_j), \hat{\boldsymbol{\theta}}_j(\hat{\mathcal{B}}_j(\hat{\mathcal{V}}_j)), \hat{\pi}_j$ and final posterior probabilities $r_{i,j}^{(final)}$ for $i = 1, \dots, n$ and $j = 1, \dots, k$.
 - 3: **for** $j = 1, \dots, k$ **do**
 - 4: **Step I: Initial clustering assignment via a fast clustering algorithm**
 - 5: $\mathbf{x}_{(j)i_j}^{(0)} \leftarrow (x_{(j)i_j,1}^{(0)}, \dots, x_{(j)i_j,d}^{(0)})^\top$ for $i_j = 1, \dots, n_j^{(0)}$, $\sum_{j=1}^k n_j^{(0)} = n$ and $\bigcup_{\forall(j,i_j)} \mathbf{x}_{(j)i_j}^{(0)} = \bigcup_{\forall i} \mathbf{x}_i$.
 - 6: **Step II: Initial model selection based on the Step I assignment**
 - 7: **for** $p = 1, \dots, d$ **do**
 - 8: $\mathbf{x}_{p(j)}^{(0)} \leftarrow (x_{(j)1,p}^{(0)}, \dots, x_{(j)n_j^{(0)},p}^{(0)})^\top$,
 - 9: $(F_{p(j)}^{(0)}, \boldsymbol{\gamma}_{p(j)}^{(0)}) \leftarrow \arg \min_{mar, \boldsymbol{\gamma}} -2 \cdot \ell^{mar}(\boldsymbol{\gamma}; \mathbf{x}_{p(j)}^{(0)}) + |\boldsymbol{\gamma}| \cdot \log(n_j^{(0)})$, where ℓ^{mar} is the log-likelihood of the univariate distribution mar for $mar \in \{\text{candidate univariate parametric marginal distributions}\}$,
 - 10: $\mathbf{u}_{p(j)}^{(0)} \leftarrow F_{p(j)}^{(0)}(\mathbf{x}_{p(j)}^{(0)}; \boldsymbol{\gamma}_{p(j)}^{(0)})$,
 - 11: $\mathbf{u}_{(j)}^{(0)} \leftarrow (\mathbf{u}_{1(j)}^{(0)}, \dots, \mathbf{u}_{d(j)}^{(0)})^\top$,
 - 12: $\mathcal{F}_j^{(0)} \leftarrow \{F_{1(j)}^{(0)}, \dots, F_{d(j)}^{(0)}\}$,
 - 13: $\text{bicop} \in \{\text{candidate parametric pair copula families}\}$,
 - 14: $\pi_j^{(0)} \leftarrow \frac{n_j^{(0)}}{n}$,
 - 15: $\text{model}_{\text{markov}} \leftarrow \text{RVineStructureSelect}(\mathbf{u}_{(j)}^{(0)}, \text{familyset}=\text{bicop}, \text{trunclevel}=1)$, where for the component j , $\text{RVineStructureSelect}$ determines its vine tree structure truncated at tree level 1, associated pair copula families among the set bicop and its parameters as described in Section 3.2,
 - 16: $\mathcal{V}_j^{(0)} \leftarrow \text{model}_{\text{markov}}\$Matrix$, $\mathcal{B}_j^{(0)} \leftarrow \text{model}_{\text{markov}}\$Family$ and $\boldsymbol{\theta}_j^{(0)} \leftarrow \text{model}_{\text{markov}}\$pars$,
 - 17: **Step III: Parameter estimation via the ECM algorithm allowing for Markov (vine) tree structures**
 - 18: **while** $\text{stop}=\text{FALSE}$ **do**
 - 19: $t \leftarrow 0$,
 - 20: **for** $j = 1, \dots, k$ **do**
 - 21: $\mathcal{F}_j^{(t+1)} \leftarrow \mathcal{F}_j^{(0)}$, $\mathcal{V}_j^{(t+1)} \leftarrow \mathcal{V}_j^{(0)}$, $\mathcal{B}_j^{(t+1)} \leftarrow \mathcal{B}_j^{(0)}$,
 - 22: Update $r_{i,j}^{(t+1)}$ as in Equation (17) for $i = 1, \dots, n$,
 - 23: Update $\pi_j^{(t+1)}$, $\boldsymbol{\gamma}_j^{(t+1)}$ and $\boldsymbol{\theta}_j^{(t+1)}$ sequentially as in Equations (19), (21) and (22), respectively,
 - 24: $t \leftarrow t + 1$,
 - 25: **if** the termination criterion in Equation (23) holds **then**
 - 26: $s \leftarrow t$, $\text{stop}=\text{TRUE}$ and **break**.
-

27: **Step IV: Temporary clustering assignment based on the Markov (vine) tree structure**

28: $\mathbf{x}_i \in \mathcal{C}_{j^*} \iff j^* = \arg \max_{j=1, \dots, k} r_{i,j}^{(s)}$ for $i = 1, \dots, n$.

29: **for** $j = 1, \dots, k$ **do**

30: $\mathbf{x}_{(j)i_j}^{(s)} \leftarrow (x_{(j)i_j,1}^{(s)}, \dots, x_{(j)i_j,d}^{(s)})^\top$ for $i_j = 1, \dots, n_j^{(s)}$, $\sum_{j=1}^k n_j^{(s)} = n$ and $\bigcup_{\forall (j,i_j)} \mathbf{x}_{(j)i_j}^{(s)} = \bigcup_{\forall i} \mathbf{x}_i$.

31: **Step V: Final model selection based on a full vine specification**

32: Perform lines 7–12 with the new assignment $\mathbf{x}_{(j)i_j}^{(s)}$ and change the iteration index from (0) to (s),

33: $model_{VCMM} \leftarrow \text{RVineStructureSelect}(\mathbf{u}_{(j)}^{(s)}, \text{familyset=bicop}, \text{trunclevel=d-1})$,

34: $\mathcal{V}_j^{(s)} \leftarrow model_{VCMM}\$Matrix$, $\mathcal{B}_j^{(s)} \leftarrow model_{VCMM}\$Family$ and $\boldsymbol{\theta}_j^{(s)} \leftarrow model_{VCMM}\$pars$.

35: **Step VI: Final clustering assignment based on the full vine specification**

36: $\mathbf{x}_i \in \mathcal{C}_{j^*} \iff j^* = \arg \max_{j=1, \dots, k} r_{i,j}^{(s+1)}$ for $i = 1, \dots, n$, where $r_{i,j}^{(s+1)}$ are the posterior probabilities calculated from the final model,

37: $\hat{\mathcal{F}}_j \leftarrow \{F_{1(j)}^{(s)}, \dots, F_{d(j)}^{(s)}\}$, $\hat{\boldsymbol{\gamma}}_j \leftarrow \{\gamma_{1(j)}^{(s)}, \dots, \gamma_{d(j)}^{(s)}\}$, $\hat{\mathcal{V}}_j \leftarrow \mathcal{V}_j^{(s)}$, $\hat{\mathcal{B}}_j(\hat{\mathcal{V}}_j) \leftarrow \mathcal{B}_j^{(s)}$, $\hat{\boldsymbol{\theta}}_j(\hat{\mathcal{B}}_j(\hat{\mathcal{V}}_j)) \leftarrow \boldsymbol{\theta}_j^{(s)}$, $\hat{\pi}_j \leftarrow \pi_j^{(s)}$, $r_{i,j}^{(final)} \leftarrow r_{i,j}^{(s+1)}$.

5. Simulation studies

This section will demonstrate the remarkable and promising results of our clustering algorithm, VCMM, using simulated data. We compare its performance with the initial partition from k-means to some well-known model-based clustering algorithms: the mixture of multivariate normal, skew normal, t, and skew t distributions. We fit the mixture of multivariate normal distributions using the package `mclust` and the others using the package `mixsmsn`. The latter fits scale mixtures of skew normal distributions and works with the initial partition of k-means like our algorithm. Therefore, the comparison of the performance of the VCMM and the chosen competing algorithms is fairer. We work with the default specifications of the packages but specify the total number of clusters and seed. For the clustering performance evaluation, we use the BIC value and misclassification rate when the true labels are available. The lower the BIC value or misclassification rate, the better the clustering assignment.

The BIC criterion compares only models studied; thus, it selects a better model among the evaluated ones. However, it does not imply that it selects the best model. Since unsupervised learning problems do not contain the true labels of the observations, a separation of the data in training and test sets is not feasible. Therefore, the misclassification rate that we consider can be regarded as the in-sample misclassification rate of supervised learning.

In Sections 5.1 and 5.2, the simulated data has three variables, two clusters, either 100 or 500 observations in each cluster, and we replicate their data generating process 100 times. $X_{p(1)} = F_{p(1)}^{-1}(U_{p(1)}; \boldsymbol{\gamma}_{p(1)})$ and $X_{p(2)} = F_{p(2)}^{-1}(U_{p(2)}; \boldsymbol{\gamma}_{p(2)})$ for $p = 1, 2, 3$ give the variables of the first and second clusters, respectively. We

simulate $U_{p(1)}$ and $U_{p(2)}$ from a specified vine copula model and specify $F_{p(1)}, F_{p(2)}, \gamma_{p(1)}, \gamma_{p(2)}$. A mixture of vine copulas generates the first scenario in Section 5.1 with one/two parameter pair copula families and non-Gaussian margins. Section 5.2 simulates data from a mixture of vine copulas with single parameter pair copulas and Gaussian/non-Gaussian margins. In the first scenario, we aim to analyze how well the VCMM improves the clustering compared to its starting partition from k-means. In the second scenario, we aim to analyze how well the VCMM and other model-based clustering algorithms capture different dependence structures and shapes hidden in the multivariate data with different numbers of observations.

In Section 5.3, we discuss the effect of different initial clustering techniques at Step I in Algorithm 1 on the VCMM using the artificial data from a mixture of vine copulas with Gaussian copulas and Gaussian margins. In Section 5.4, we aim to analyze the performance of the VCMM when the data generating process is misspecified, e.g., we simulate the data from a mixture of multivariate skew t distributions.

5.1. The mixture of vine copulas with one/two parameter pair copulas and non-Gaussian margins

We simulate data $U_{p(1)}$ and $U_{p(2)}$ for $p = 1, 2, 3$ from a vine copula model, where pair copula families have either single or two parameters, as shown in Figure 4. Both clusters include positive as well as high, medium, and low strength dependencies.

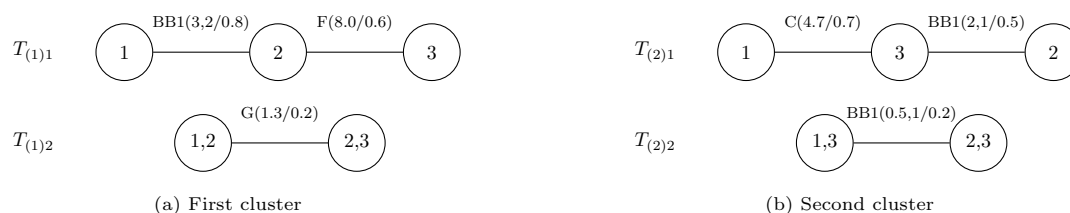


Figure 4: Vine tree structure of simulated data with one/two parameter pair copulas and two clusters. A letter at an edge refers to its bivariate copula family, where C: Clayton, G: Gumbel, F: Frank, and BB1: BB1 copula. The true parameter value(s) and corresponding Kendall's τ of the pair copula are given inside the parenthesis (parameter(s)/Kendall's τ).

Then we transform the data from u-scale $U_{p(1)}, U_{p(2)}$ to x-scale $X_{p(1)}, X_{p(2)}$ as explained in Section 5. Table 1 presents the marginal distributions with the parameters. The clusters are non-Gaussian.

$F_{1(1)}(\gamma_{1(1)})$	$F_{2(1)}(\gamma_{2(1)})$	$F_{3(1)}(\gamma_{3(1)})$	$F_{1(2)}(\gamma_{1(2)})$	$F_{2(2)}(\gamma_{2(2)})$	$F_{3(2)}(\gamma_{3(2)})$
$llogis(1.5, 1.25)$	$exp(0.1)$	$lnorm(0.1, 1.3)$	$lnorm(2.5, 0.5)$	$logis(5, 3)$	$exp(0.05)$

Table 1: Univariate marginal distributions and associated parameters of each cluster. They are defined in Appendix A.

We evaluate the clustering performance of the VCMM and k-means, visualizing the misclassification rate per simulation replication in box plots. For the larger number of observations (500 observations per cluster), Figure 5 shows that the VCMM provides a noticeably better fit than k-means. On average, it improves the accuracy by 22% compared to its initial partition. For the small number of observations (100 observations

per cluster), its average misclassification rate is 10% less than k-means, but the VCMM variance in the accuracy increases as the number of observations gets lower. The VCMM requires, on average, 25 and 17 ECM iterations for the large and small numbers of observations, respectively, i.e., the convergence takes more iterations with a larger data set here.

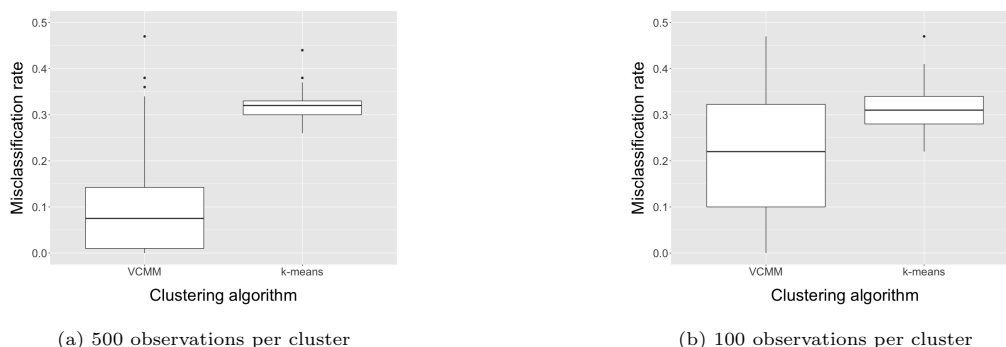


Figure 5: Comparison of the clustering performance of the VCMM and its initial partition algorithm k-means over 100 replications under the scenario specified in Figure 4 and Table 1.

5.2. The mixture of vine copulas with one parameter pair copulas and Gaussian/non-Gaussian margins

In this scenario, we work with single parameter pair copulas, add Gaussian margins within the clusters, simulate data on u-scale $U_{p(1)}, U_{p(2)}$ for $p = 1, 2, 3$ from the vine tree structures shown in Figure 6. Both clusters share the same vine tree structure and include asymmetric tail dependencies. The second cluster has a symmetric, non-Gaussian dependency (Frank copula) between the variables $U_{1(2)}$ and $U_{2(2)}$.

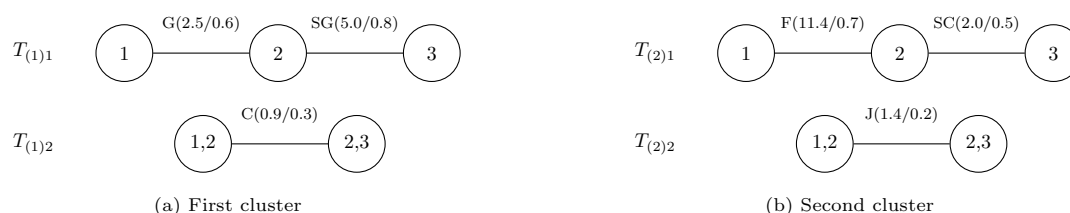


Figure 6: Vine tree structure of simulated data with two clusters. A letter at an edge refers to its bivariate copula family, where C: Clayton, SC: Survival Clayton, G: Gumbel, SG: Survival Gumbel, F: Frank, and J: Joe copula. The true parameter value and corresponding Kendall's τ of the pair copula are given inside the parenthesis (parameter/Kendall's τ).

The next step is to obtain the data on the x-scale $X_{p(1)}, X_{p(2)}$ as described before. Marginal distributions and the parameters used are listed in Table 2. We illustrate simulated data (500 observations per cluster) on the x-scale in the left panel of Figure 7, where a color represents the observations from a cluster. The generated clusters are non-elliptical. The fitted VCMM detects the true shape of the clusters as shown in the right panel of Figure 7 as opposed to other model-based clustering algorithms given in Figure 1.

$F_{1(1)}(\gamma_{1(1)})$	$F_{2(1)}(\gamma_{2(1)})$	$F_{3(1)}(\gamma_{3(1)})$	$F_{1(2)}(\gamma_{1(2)})$	$F_{2(2)}(\gamma_{2(2)})$	$F_{3(2)}(\gamma_{3(2)})$
$\mathcal{N}(1, 2)$	$exp(0.2)$	$lnorm(0.8, 0.8)$	$lnorm(1.5, 0.4)$	$\mathcal{N}(18, 5)$	$exp(0.2)$

Table 2: Univariate marginal distributions and associated parameters of each cluster. They are defined in [Appendix A](#).

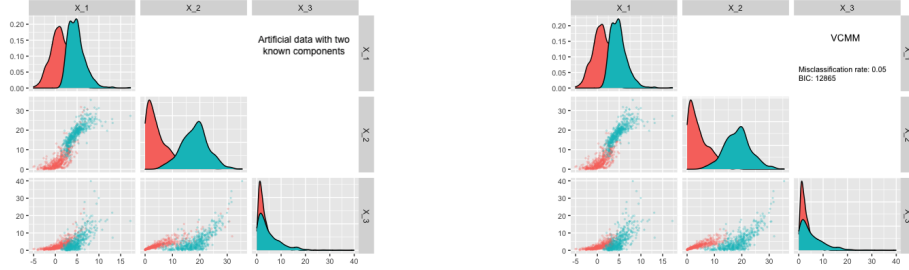


Figure 7: Pairwise scatter plot of simulated data (500 observations per cluster) on x-scale under the scenario specified in [Figure 4](#) and [Table 1](#) (left). The right plot shows the fitted VCMM. The red and green points show the observations of one cluster and the other cluster, respectively. The diagonal of the plots shows each cluster’s associated variable’s marginal density function.

[Figure 8](#) visualizes the misclassification rate and BIC value per simulation replication in box plots for 500 observations per cluster. The VCMM is superior to other model-based clustering algorithms regarding both the misclassification rate and the BIC value. It separates two non-elliptical clusters adequately as expected, whereas others tend to find it challenging. Even though they cannot model two clusters as the VCMM does, the mixtures of multivariate skew distributions show a better fit than elliptical distributions in terms of the BIC value. The mean misclassification rate of the mixtures of multivariate skew t distributions and that of the VCMM are 4% and 8% less than that of multivariate normal distributions.

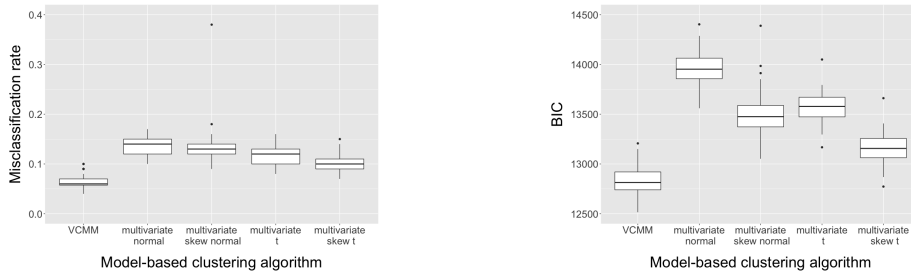


Figure 8: Comparison of the model-based clustering algorithms’ performance over 100 replications with 500 observations per cluster under the scenario specified in [Figure 6](#) and [Table 2](#).

[Figure 9](#) shows that the misclassification rates of the VCMM do not change enormously for 100 observations per cluster and are still lower than the others. Its variance in the accuracy increases with the smaller number of observations as in the first simulation scenario. The BIC values favor the VCMM, and after the VCMM, the mixtures of multivariate skew distributions provide better fits than the others.

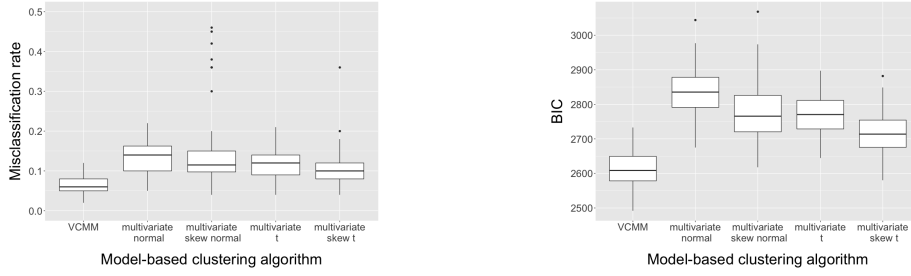


Figure 9: Comparison of the model-based clustering algorithms' performance over 100 replications with 100 observations per cluster under the scenario specified in Figure 6 and Table 2.

5.3. The mixture of vine copulas with Gaussian copulas and Gaussian margins: significant overlaps

We generate artificial data from a mixture of two vine copulas as specified in Appendix C. They have only Gaussian copulas between the pairs of variables, and each margin follows a univariate normal distribution. Thus, the scenario represents a mixture of multivariate normal distributions. We do not observe strong multimodality of variables in the diagonal of the left panel in Figure 10. However, the data has two obvious clusters with many overlaps, creating a x shape in three dimensions, in the right panel of Figure 10.

In an attempt to determine the true groups, we fit the VCMM as in previous simulation studies. Since k-means assumes spherical shapes of clusters, we suspect that the VCMM's model selection using the initial partition from k-means could be satisfactory in such a scenario. The VCMM results in 65% classification accuracy with the BIC of 12447. As we suggest at Step I in Algorithm 1, other partition strategies can be used before fitting the VCMM. For instance, we partition the data by the model-based hierarchical clustering using the function `hcVVV` with its default specifications in the package `mclust` and then run our algorithm. As a result, the VCMM has 95% classification accuracy with the BIC of 12039. Therefore, using different starting partitions in the VCMM and selecting a final model with the lowest BIC are suggested. Also, fitting the mixture of multivariate normal distributions gives 96% classification accuracy with the BIC of 11987.

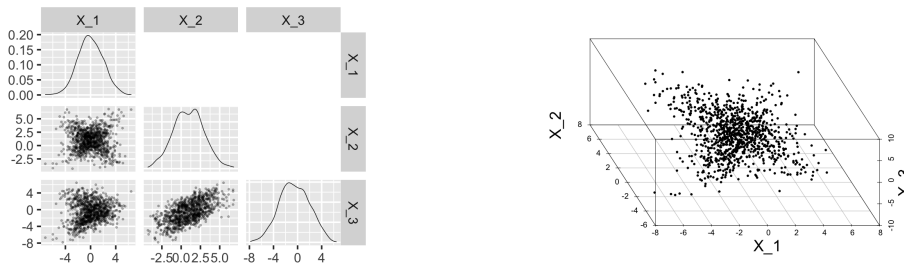


Figure 10: Pairwise(left) and 3-dimensional scatter plot(right) of artificial data (500 observations per cluster) on x-scale under the scenario specified in Figure C.17 and Table C.7. The diagonal of the plot on the left shows the corresponding variable's marginal density function.

To conclude, the VCMM does show its effectiveness and flexibility in clustering multivariate non-Gaussian

and Gaussian data in our simulation studies when the data generating process is a mixture of vine copulas. Even though its starting partition cannot reasonably identify the clusters, the VCMM often deals with them.

5.4. The mixture of multivariate skew t distributions

As a misspecification scenario, we simulate data in three dimensions with two components from the mixture of multivariate skew t distributions expressed as a class of skew normal independent distributions (Cabral et al., 2012). The total number of observations is 1000. Denoting the density of a multivariate skew t distribution by $ST(\cdot; \boldsymbol{\mu}, \boldsymbol{\Sigma}, \boldsymbol{\lambda}, \nu)$ with location vector $\boldsymbol{\mu}$, scale matrix $\boldsymbol{\Sigma}$, skewness vector $\boldsymbol{\lambda}$, and degrees of freedom ν , assume a random vector \mathbf{X} has this mixture distribution. Then its density at \mathbf{x} is given by

$$\pi_1 \cdot ST(\mathbf{x}; \boldsymbol{\mu}_1, \boldsymbol{\Sigma}_1, \boldsymbol{\lambda}_1, \nu_1) + (1 - \pi_1) \cdot ST(\mathbf{x}; \boldsymbol{\mu}_2, \boldsymbol{\Sigma}_2, \boldsymbol{\lambda}_2, \nu_2), \quad (24)$$

where the true values of the parameters used in the simulation are $\boldsymbol{\mu}_1 = (1, 1, 0)^\top$, $\boldsymbol{\mu}_2 = (-2, -2, -2)^\top$, $\pi_1 = 0.6$, $\boldsymbol{\lambda}_1 = (4, -4, 4)^\top$, $\boldsymbol{\lambda}_2 = (-4, 4, 4)^\top$, $\nu_1 = 8$, $\nu_2 = 10$, and $\boldsymbol{\alpha}_1 = \boldsymbol{\alpha}_2 = (2, 1, 1, 2, 1, 2)$ vectorizing the upper triangular matrix of symmetric matrices $\boldsymbol{\Sigma}_1 = \boldsymbol{\Sigma}_2$. We replicate the data generating process 100 times, and Table 3 shows that the mixture of multivariate skew t distributions fits well with the data as expected. The mixture of multivariate normal distributions has more difficulty in capturing non-elliptical components than the VCMM. All in all, the VCMM has good credibility also under this scenario.

Mixture model	Multivariate skew t	VCMM	Multivariate normal
Average misclassification rate	0.06	0.09	0.13
Average BIC	10676	10822	10881
Average log-likelihood	-5248	-5330	-5380

Table 3: Comparison of the model-based clustering algorithms' performance over 100 replications with 1000 observations under the scenario specified in Equation (24). The best result in each row is highlighted.

6. Real data sets

This section illustrates the VCMM's usefulness in analyzing and clustering multivariate non-Gaussian real data. We first focus on improvements the VCMM provides thanks to its steps given in Algorithm 1. Later, we analyze the effect of using a fixed vine tree structure for clusters in the VCMM and compare its performance with other models. We run other clustering algorithms using the same random seed for a fair comparison, thereby using the same starting partitions (except the mixture of multivariate normal distributions). We report their results regarding the misclassification rate and BIC value as in the simulation studies in Section 5.

Additionally, we will discuss the computational effort of the VCMM. All computations are run on a MacBook Air (2018) with a 1,6 GHz Dual-Core Intel Core i5 and 8 GB of RAM, running R version 4.0.3. Section 6.3 will also study the issue of determining the optimal number of clusters in the VCMM.

6.1. AIS

A well-analyzed Australian Institute of Sport (AIS) data consists of 13 measurements made on 102 male and 100 female athletes. Our objective of clustering this data is to see if the VCMM can find two clusters for females and males and analyze its steps' performance. For our analysis, we select a subset of five variables: lean body mass (LBM), weight (Wt), body mass index (BMI), white blood cell count (WBC), and percentage of body fat (PBF). This sample appears non-Gaussian and has asymmetric dependence patterns shown on the bottom panels in Figure 11. To obtain u-data, we fit the empirical cumulative distribution function of each variable in each class. The lower panels in pairs plots show normalized contour plots, and we often do not observe Gaussian dependence since most contours are non-elliptical. The pairwise dependence between the same pair of variables usually is the same in females and males, but its strength is different (e.g., Wt and BMI). The marginal density function of BMI and WBC for both classes is similar to each other as shown in the diagonal of the top left panel in Figure 11.

Fitting k-means with 10000 different seeds leads to two different partitions of the data set. We fit the VCMM using both partitions but present the result for the best VCMM, whose BIC value is lower than the other. However, both models have the same final accuracy.

Since we know the gender of each observation, we can evaluate the misclassification rate of the binary classification for the clustering algorithm and associate the final clusters with the classes. The VCMM improves its clustering power with its steps in Algorithm 1 as shown in Table 4. The starting partition obtained from k-means assigns almost one-fourth of males to females (Step I). Then Step II fits the initial VCMM model using Markov trees, thereby returning a log-likelihood value. The accuracy is eight percent higher than the starting partition. After the ECM iterations and temporary clustering assignment (Step III and Step IV), the VCMM reduces the misclassification rate by 12% compared to k-means. Selecting the final VCMM with a full vine specification (Step V and Step VI) provides a crucial gain in the log-likelihood. In the end, the VCMM identifies almost all females correct except one female. Overall it provides 12% higher accuracy in revealing females and males than k-means. The misclassified observations by the VCMM lie on the boundary of the classes as shown in the top right panel of Figure 11.

Clustering algorithm	k-means		VCMM after Step II (with Markov trees)		VCMM after Step IV (ECM using Markov trees)		final VCMM (Full vine using Step IV's assignment)	
	1	2	1	2	1	2	1	2
Gender								
Female	93	7	95	5	100	0	99	1
Male	26	76	12	90	8	94	7	95
Misclassification rate	0.16		0.08		0.04		0.04	
Log-likelihood	-		-2688		-2603		-2326	

Table 4: Comparison of the VCMM's steps' clustering performance on the subset of AIS data.

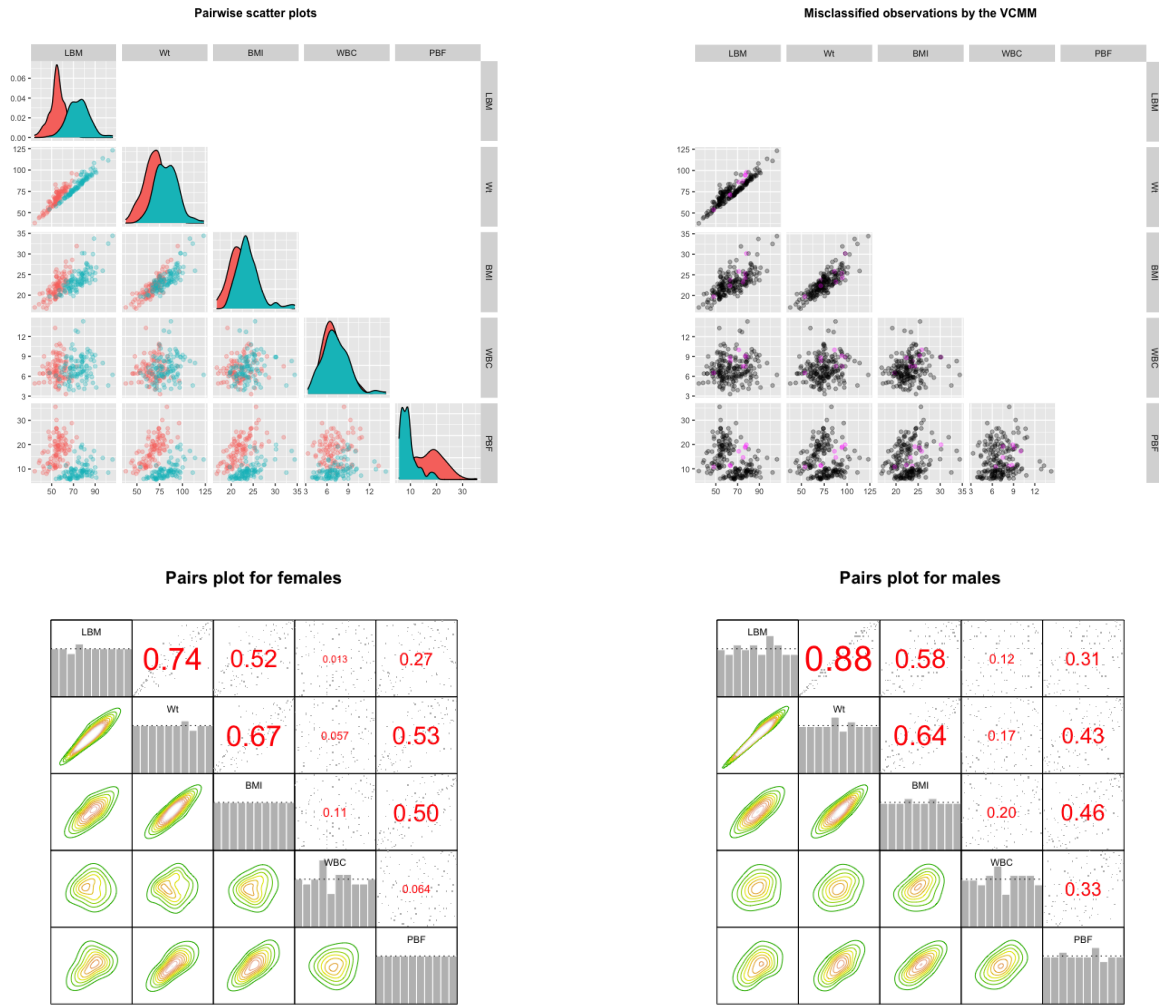


Figure 11: Pairwise scatter plot of the subset of AIS data (top left) with red points for observations of females and green points for males, where diagonal: marginal density function of each class's corresponding variable, and of the misclassified observations by the VCMM shown by magenta (top right). Pairs plots of females (bottom left) and males (bottom right), where upper: pairs plots of copula data, diagonal: histogram of copula margins, lower: normalized contour plots.

Figure 12 illustrates the estimated vine copula models' first tree level by the final VCMM. The estimated vine tree structure is not the same for females and males. It is a path, i.e., D-vine, for males. The estimated pairwise dependence between pairs of the variables is non-Gaussian with diverse dependence strengths in females and males, except the pair of Wt and BMI. For instance, the pair of the variables, PBF and Wt, shows high strength, non-Gaussian dependence (Survival BB8 copula) in females. Appendix D presents all estimated model components and parameters by the VCMM. In higher tree levels, the highest (absolute value) estimated Kendall's τ for females is 0.74 and exists in the second tree, while 0.76 in the third tree for males, i.e., high strength conditional dependence exists in the higher tree levels. The VCMM fits a

log-logistic distribution for BMI in both clusters, while other variables' marginal distributions are different in males and females. The VCMM runs for 2.28 minutes, and the ECM iterations stop after 15 iterations.

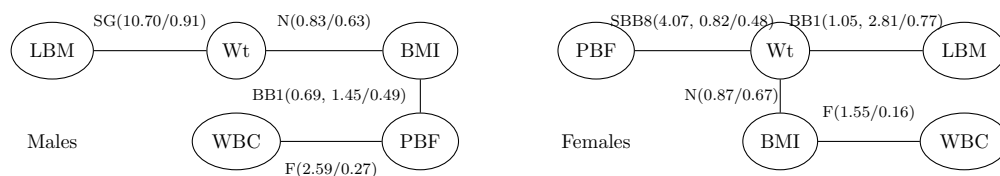


Figure 12: The first tree level of the estimated vine copula model for females and males. A letter at an edge with numbers inside the parenthesis refers to its bivariate copula family with its estimated parameter(s)/Kendall's $\hat{\tau}$, where N: Gaussian, SG: Survival Gumbel, F: Frank, BB1: BB1, and SBB8: Survival BB8 copula.

Figure 13 shows the QQ plots of the variables in both fitted clusters. The fitted univariate marginal distributions by the VCMM are adequate for the female cluster. However, the margin selection could be improved for the variables BMI and PBF in the male cluster. For instance, adding univariate skew t distribution into the candidate list of univariate marginal distributions in line 9 of Algorithm 1 could be considered.

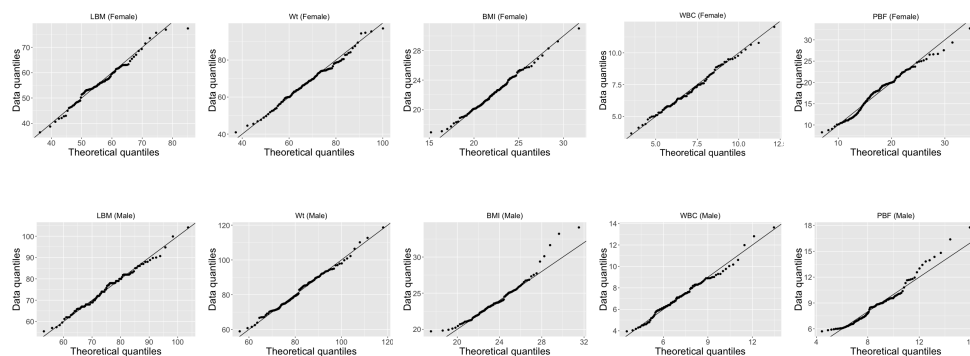


Figure 13: QQ plots of the variables in female (top) and male (bottom) clusters by the VCMM.

6.2. Breast Cancer Wisconsin (Diagnostic)

We now illustrate the effect of using a fixed vine tree structure for clusters in the VCMM and compare their performance with other model-based clustering algorithms. We specify each cluster's vine tree structure as a star, i.e., C-vine, in the VCMM, selecting their root node with our approach explained in Section 3.2, and denote this model by VCMM(C-vine). We assess their performance on the Breast Cancer Wisconsin (Diagnostic) data obtained from the UCI Machine Learning data repository (Dheeru & Karra Taniskidou, 2017), where a digitized image of a fine needle aspirate (FNA) of a breast mass (Mangasarian et al., 1995) is used to have ten features from 569 patients. The mean value, extreme value (mean of the three largest

values), and standard error of each feature are calculated, returning 30 continuous variables. The data contains two types of diagnosis: benign (352 patients) and malignant (212 patients), enabling us to assess the misclassification rate of the binary classification for the algorithms. We limit this illustration to a subset of four variables: perimeter standard error (PSE), extreme smoothness (ES), extreme concavity (EC), and extreme concave points (ECP) shown on the left panel in Figure 14. The data has non-Gaussian variables like PSE. We fit two-component clustering models to the data, and k-means is not sensitive to seeds.

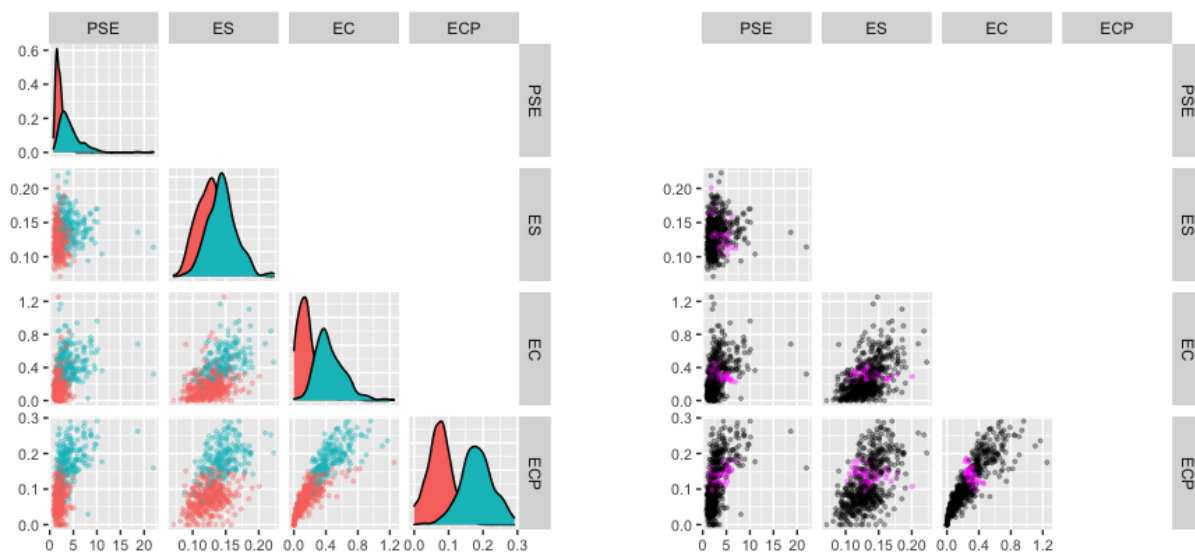


Figure 14: Pairwise scatter plots of the subset of Breast Cancer Wisconsin (Diagnostic) data. On the left panel, red/green points denote observations of benign/malignant. The right panel shows the VCMM clustering result, where magenta points show observations whose estimated posterior probability is smaller than 0.9 in their assigned cluster.

Table 5 shows that the VCMM provides a noticeably better clustering performance than other candidates. Even though its number of free parameters is higher than the mixture of multivariate normal distributions, not only does it achieve a lower BIC value, but the misclassification rate is also lower than theirs. The flexibility of the VCMM to model different dependence structures and marginal densities makes the difference. The selected vine tree structure by the VCMM is a path for the malignant cluster and a star with the root node of the variable ECP for the benign cluster. It runs for 1.07 minutes, and the ECM iterations stop after nine iterations. The right panel in Figure 14 shows that the observations whose estimated posterior probability is smaller than 0.9 in their assigned cluster are at the border of the support regions of benign and malignant. Appendix E gives its estimated model components and the QQ plots of the fitted margins.

Moreover, imposing a fixed vine structure in the VCMM, VCMM(C-vine), decreases the model power, where the selected root node is the variable ECP for both clusters. It appears to be the best vine copula mixture model regarding the BIC value. However, its misclassification rate is higher than the VCMM. Thus, we would need to construct a better model comparison criterion than the BIC value in the vine copula

mixture model context in the future. The VCMM(C-vine) takes 7.14 minutes and 57 ECM iterations.

Mixture model	VCMM	VCMM (C-vine)	Multivariate normal	Multivariate skew normal	Multivariate t	Multivariate skew t
Misclassification rate	0.10	0.18	0.12	0.15	0.11	0.15
BIC	-3970	-4014	-3664	-3785	-3727	-3858
Number of free parameters	32	31	29	37	30	38

Table 5: Comparison of model-based clustering algorithms’ performance on the subset of Breast Cancer Wisconsin (Diagnostic) data. The best result in each row is highlighted.

6.3. Sachs Protein

We consider the Sachs Protein data analyzed by [Sachs et al. \(2005\)](#). It consists of logarithmized levels of 11 phosphorylated proteins and phospholipids in individual cells, subjected to general and specific molecular interventions. The original goal is to learn the causal pathways linking a set of 11 proteins and compare them to the known links in the literature, thereby validating the important model tools in genetics, Bayesian networks. The data is continuous as shown in the left panel of [Figure 15](#), where we work with 6161 observations from nine experiments (*b2camp*, *cd3cd28*, *cd3cd28 + aktinhib*, *cd3cd28 + g007*, *cd3cd28 + ly*, *cd3cd28 + psitect*, *cd3cd28 + u0126*, *cd3cd28icam2*, *pma*) after removing 1305 observations with zero values to avoid dealing with zero inflation. The standard approach in the literature is to assume that the data follows a multivariate Gaussian distribution, thereby formulating a Gaussian Bayesian network (GBN). However, [Figure 15](#) shows that the data has non-Gaussian univariate distributions and different components. Accordingly, [Zhang & Shi \(2017\)](#) works with the two-component Gaussian mixture copula Bayesian network and detects the underlying causal links better than the GBN.

Even though bimodality exists for some variables, such as PIP2 and mek, and there are two obvious groups on some scatter plots like the one of Akt and PKA, it is unclear how many hidden components exist in the data. Therefore, following our suggestion in the previous sections, we fit the VCMM using a starting partition of k-means and model-based hierarchical clustering with two to eleven components. [Figure 16](#) shows that using the initial partition from model-based hierarchical clustering in the VCMM suggests having ten components because it is the global minimum point of its plot. However, starting with the assignment of k-means points out nine components in the experiments, giving the lowest BIC value among the evaluated ones. Thus, we select it as our final VCMM model. [Table 6](#) shows that most observations of the experiments *b2camp*, *cd3cd28 + g007*, *cd3cd28 + psitect*, *cd3cd28 + u0126* are revealed as a cluster. The remaining five experiments’ observations usually belong to the other four clusters. Their partition is given in the right panel of [Figure 15](#). The fitted univariate marginal distributions and bivariate copula families are mostly non-Gaussian in the clusters, showing the need for a non-Gaussian model. The fitted VCMM is available from the authors upon request.

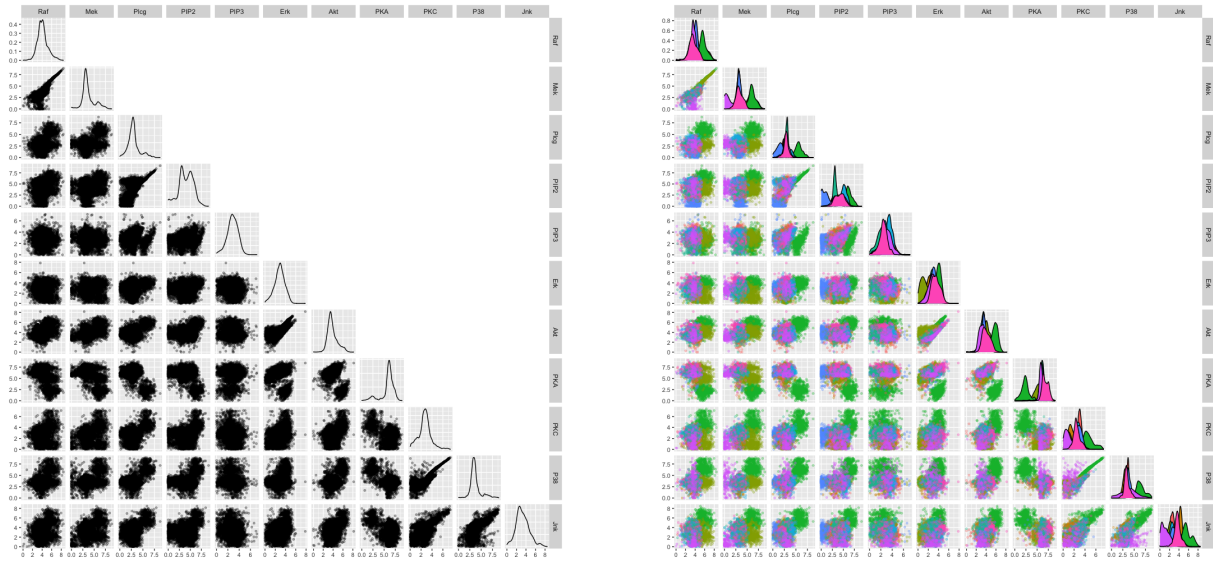
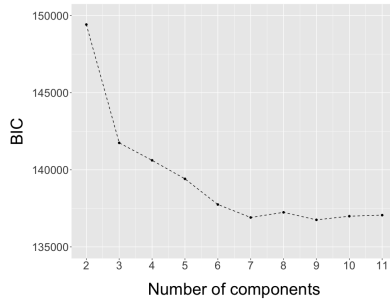
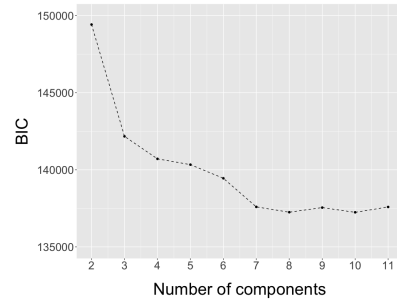


Figure 15: Pairwise scatter plots of the Sachs Protein data (left) and its partition by the VCMM (right). The diagonal of the plots shows the corresponding variable's marginal density function in each cluster.



(a) VCMM with k-means



(b) VCMM with model-based hierarchical clustering

Figure 16: BIC values for the VCMM with different starting partitions and number of components on the Sachs Protein data.

Experiment	<i>b2camp</i>	<i>cd3cd28</i>	<i>cd3cd28 + aktinhib</i>	<i>cd3cd28 + g007</i>	<i>cd3cd28 + ly</i>	<i>cd3cd28 + psitect</i>	<i>cd3cd28 + u0126</i>	<i>cd3cd28icam2</i>	<i>pma</i>
1	0	245	297	0	298	62	0	14	5
2	0	201	36	0	145	37	4	26	33
3	0	3	2	0	0	1	500	0	1
4	0	0	0	695	0	0	0	0	0
Cluster 5	3	143	36	0	125	6	2	246	310
6	4	170	405	0	168	8	0	203	198
7	0	23	39	0	42	473	1	8	25
8	147	12	15	0	8	7	1	22	13
9	1	20	15	0	15	10	0	344	288

Table 6: Clustering result for the VCMM with nine components using the starting partition of k-means on the Sachs Protein data.

7. Conclusion

We propose a vine copula mixture model that works with continuous data and fits all classes of vine tree structures. It uses parametric marginal distributions and pair copula families. It applies a wide range of pair copula families; thus, it accommodates diverse tail dependence and asymmetries within the components. Due to its parametric nature, it nicely interprets the structure of the data. Assuming the number of components in the data is known, we follow a data-driven approach for the remaining model selection problems. We work with the ECM algorithm for parameter estimation. With the proposed method, we formulate a new model-based clustering algorithm called VCMM.

We evaluate the performance of the algorithm on simulated and real data. Our simulation studies illustrate that the vine copula based clustering has greater flexibility than various model-based clustering algorithms available in the literature and hence captures the non-Gaussian components hidden in the data better than others, especially when the data has heavy-tailed margins and tail dependence between pairs of variables. The real data analysis supports it and the better clustering assignment thanks to allowing all types of vine tree structures. Due to its flexibility in the formulation, it can also capture Gaussian components. Additionally, it can answer whether the dependence between a pair of variables changes with the variables' different values or differs among the clusters. It is an appealing clustering approach since the era of big data comes with different data characteristics.

To provide guidelines on the number of components to consider, we give a first analysis based on the BIC criterion. It turns out that the initial partition impacts the final model. Therefore, one possible future research direction is the selection of the number of components in the vine copula mixture models. It can be combined with the construction of a model comparison criterion. The ideas for sparse model selection in [Nagler et al. \(2019a\)](#) can be a starting point.

While the current algorithm has significant advancement in revealing non-elliptical components, further development would modify the proposed method to obtain parsimonious vine copula mixture models and then use them for clustering. On the one hand, the optimal truncation level can be studied, and, on the other hand, the parsimonious vine factor specification of [Krupskii & Joe \(2013\)](#) can be considered.

A potential drawback of the proposed method is the computational cost for high-dimensional data. This paper is an initial framework for using vine copulas with finite mixture models and clustering. Therefore, another future research direction is to handle variable selection and dimensionality reduction for vine copula based clustering. The traditional variable selection methods for other model-based clustering algorithms have to be reviewed and adjusted (e.g., [Raftery & Dean \(2006\)](#), [Maugis et al. \(2009\)](#)). Furthermore, the performance of the ECM algorithm's extensions, such as the expectation conditional maximization of either algorithm ([Liu & Rubin, 1994](#)), can be analyzed for our framework.

We show that different quick clustering methods can initialize the algorithm, and the final model can

differ accordingly. Since running the algorithm until the stopping condition holds takes time with high-dimensional data, initialization approaches for the vine copula mixture models need to be further improved in the future. [Scrucca & Raftery \(2015\)](#) studies a similar problem with regard to the initial parameter values in multivariate normal mixture models. Initializing the algorithm could be further studied for harder situations with significant overlaps among the components and an unknown number of components.

The proposed method can be extended to deal with mixed discrete/continuous variables and missing data as other future research directions. The construction defined in [Panagiotelis et al. \(2012\)](#) and further studied in [Panagiotelis et al. \(2017\)](#) can be a starting point for the former. [Wang & Lin \(2015\)](#) discusses how to handle missing data in multivariate skew t mixture models.

Acknowledgements

This research has been supported by the German Research Foundation (DFG grant CZ 86/6-1). We are grateful to two anonymous referees and special issue editors for comments leading to a considerably improved contribution.

Appendix A. Abbreviation for univariate marginal distributions

$lnorm(\mu, \sigma)$: log-normal distribution with mean/standard deviation parameters μ/σ on the logarithmic scale,

$exp(\lambda)$: exponential distribution with rate parameter λ ,

$llogis(\alpha, \beta)$: log-logistic distribution with shape parameter α and scale parameter β ,

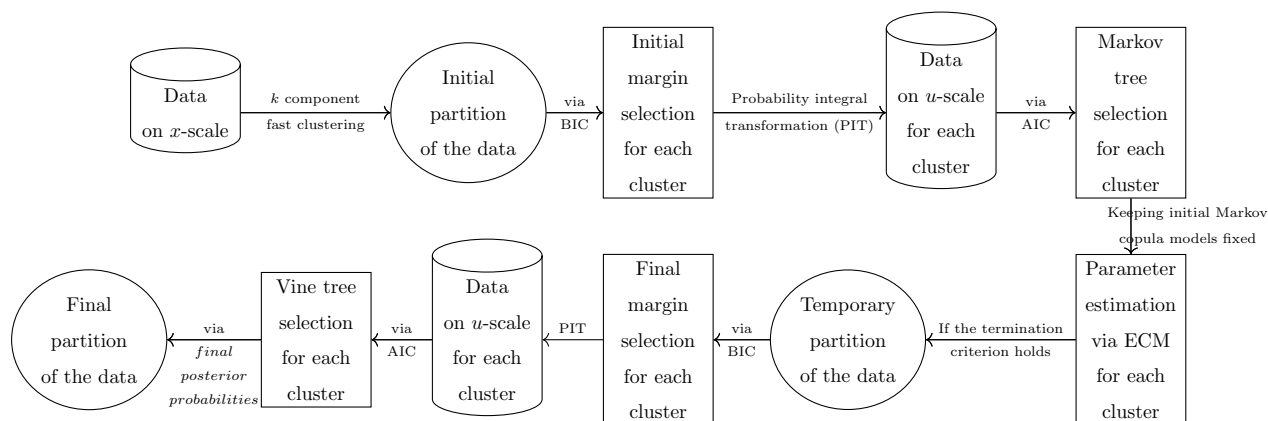
$logis(l, s)$: logistic distribution with location parameter l and scale parameter s ,

$\Gamma(\alpha, \beta)$: gamma distribution with shape parameter α and rate parameter β ,

$\mathcal{N}(\mu, \sigma)$: normal distribution with mean parameter μ and standard deviation parameter σ .

$t_3(\mu, \sigma)$: Student's t distribution with mean/standard deviation parameters μ/σ , and degrees of freedom 3.

Appendix B. Overview of the VCMM



Appendix C. Specification of the artificial data generation in Section 5.3

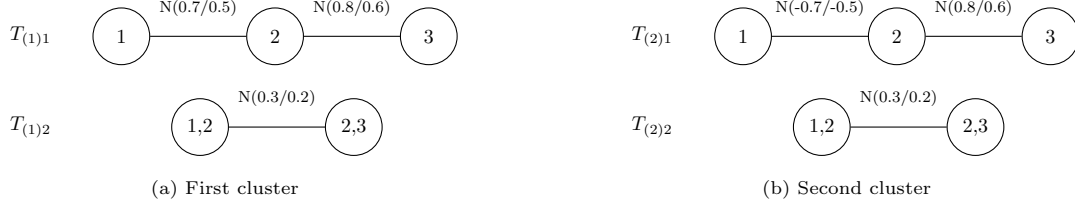


Figure C.17: Vine tree structure of simulated data with two clusters. A letter at an edge refers to its bivariate copula family, where N: Gaussian copula. The true parameter value and corresponding Kendall's τ of the pair copula are given inside the parenthesis (parameter/Kendall's τ).

$F_{1(1)}(\gamma_{1(1)})$	$F_{2(1)}(\gamma_{2(1)})$	$F_{3(1)}(\gamma_{3(1)})$	$F_{1(2)}(\gamma_{1(2)})$	$F_{2(2)}(\gamma_{2(2)})$	$F_{3(2)}(\gamma_{3(2)})$
$\mathcal{N}(0, 2)$	$\mathcal{N}(1, 2)$	$\mathcal{N}(1, 2)$	$\mathcal{N}(0, 2)$	$\mathcal{N}(1, 2)$	$\mathcal{N}(-2, 2)$

Table C.7: Univariate marginal distributions and associated parameters of each cluster. They are defined in Appendix A.

Appendix D. Estimated model components and parameters of the AIS data by the VCMM

The variable encoding is given as follows: 1: LBM, 2: Wt, 3: BMI, 4: WBC, and 5: PBF. The cluster index (1) refers to females, whereas the index (2) denotes males.

j	$\hat{F}_{1(j)}(\hat{\gamma}_{1(j)})$	$\hat{F}_{2(j)}(\hat{\gamma}_{2(j)})$	$\hat{F}_{3(j)}(\hat{\gamma}_{3(j)})$	$\hat{F}_{4(j)}(\hat{\gamma}_{4(j)})$	$\hat{F}_{5(j)}(\hat{\gamma}_{5(j)})$	$\hat{\pi}_j$
1	$llogis(12.4, 55.6)$	$\mathcal{N}(68.6, 12.1)$	$llogis(14.4, 22.0)$	$\Gamma(18.0, 2.5)$	$\Gamma(10.8, 0.6)$	0.54
2	$lnorm(4.3, 0.1)$	$lnorm(4.4, 0.1)$	$llogis(17.9, 23.5)$	$lnorm(1.9, 0.3)$	$lnorm(2.1, 0.2)$	0.46

Table D.8: Estimated mixture weight, marginal distributions and parameters of females and males. The marginal distributions are defined in Appendix A.

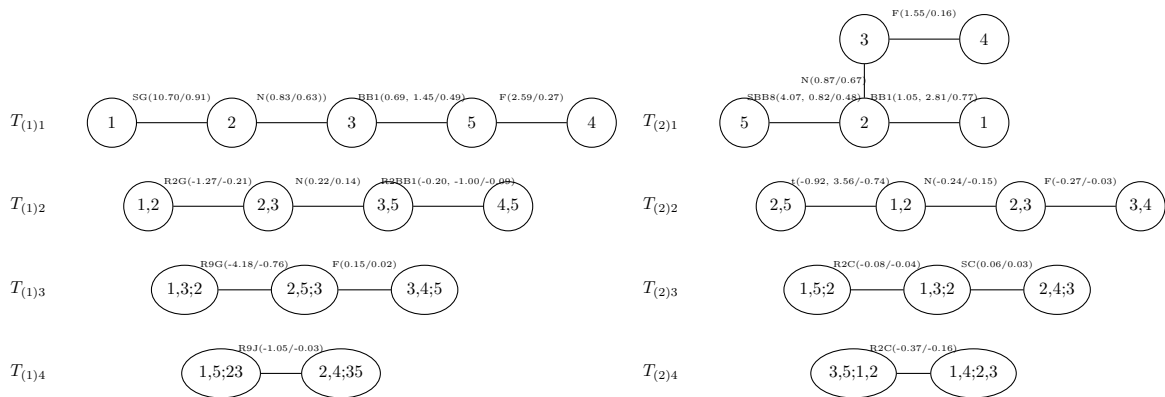


Figure D.18: Estimated vine copula models for females and males. A letter at an edge with numbers inside the parenthesis refers to its bivariate copula family with its parameter(s)/Kendall's $\hat{\tau}$, where t: t, SC: Survival Clayton, R2C: Rotated Clayton 270 degrees, R9G: Rotated Gumbel 90 degrees, R2G: Rotated Gumbel 270 degrees, R9J: Rotated Joe 90 degrees, R2BB1: Rotated BB1 270 degrees copula. Others are defined in Figure 12.

Appendix E. Estimated model components and parameters of the Breast Cancer Wisconsin (Diagnostic) data by the VCMM

The variable encoding is 1: perimeter standard error, 2: extreme smoothness, 3: extreme concavity, and 4: extreme concave points. The cluster encoding is (1): malignant and (2): benign.

j	$\hat{F}_{1(j)}(\hat{\gamma}_{1(j)})$	$\hat{F}_{2(j)}(\hat{\gamma}_{2(j)})$	$\hat{F}_{3(j)}(\hat{\gamma}_{3(j)})$	$\hat{F}_{4(j)}(\hat{\gamma}_{4(j)})$	$\hat{\pi}_j$
1	$lnorm(1.3, 0.5)$	$llogis(13.4, 0.1)$	$lnorm(-0.8, 0.3)$	$\Gamma(22.4, 118.6)$	0.35
2	$lnorm(0.7, 0.4)$	$\Gamma(43.2, 349.6)$	$\mathcal{N}(0.15, 0.1)$	$\mathcal{N}(0.07, 0.03)$	0.65

Table E.9: Estimated mixture weight, marginal distributions and parameters of benign and malignant. The marginal distributions are defined in Appendix A.

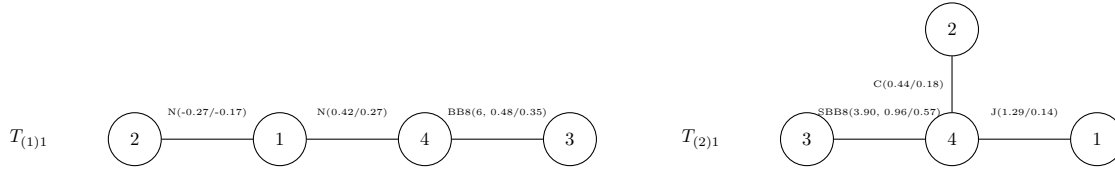


Figure E.19: The first tree level of the estimated vine copula models for benign and malignant. A letter at an edge with numbers inside the parenthesis refers to its bivariate copula family with its parameter(s)/Kendall's $\hat{\tau}$, where C: Clayton, J: Joe and BB8: BB8 copula. Others are defined in Figure 12.

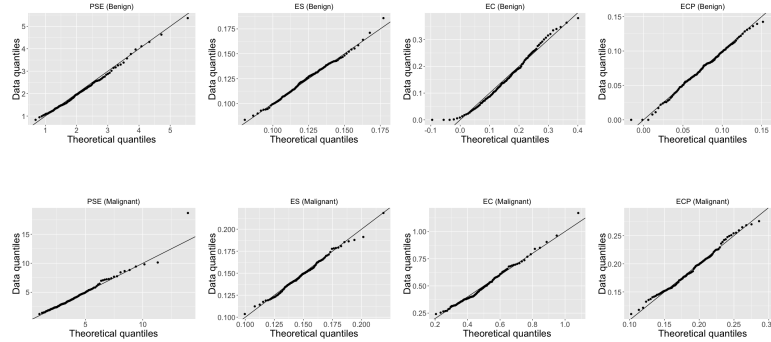


Figure E.20: QQ plots of the variables in benign (top) and malignant (bottom) clusters by the VCMM.

References

- Aas, K., Czado, C., Frigessi, A., & Bakken, H. (2009). Pair-copula constructions of multiple dependence. *Insurance: Mathematics and Economics*, 44, 182 – 198. doi:10.1016/j.insmatheco.2007.02.001.
- Akaike, H. (1998). Information Theory and an Extension of the Maximum Likelihood Principle. (pp. 199–213). doi:10.1007/978-1-4612-1694-0_15.
- Andrews, J. L., & McNicholas, P. D. (2011). Mixtures of modified t-factor analyzers for model-based clustering, classification, and discriminant analysis. *Journal of Statistical Planning and Inference*, 141, 1479 – 1486. doi:10.1016/j.jspi.2010.10.014.

- Bedford, T., & Cooke, R. M. (2001). Probability density decomposition for conditionally dependent random variables modeled by vines. *Annals of Mathematics and Artificial Intelligence*, *32*, 245–268. doi:10.1023/A:1016725902970.
- Bedford, T., & Cooke, R. M. (2002). Vines - A new graphical model for dependent random variables. *Annals of Statistics*, *30*, 1031–1068. doi:10.1214/aos/1031689016.
- Bouveyron, C., & Brunet-Saumard, C. (2014). Model-based clustering of high-dimensional data: A review. *Computational Statistics and Data Analysis*, *71*, 52–78. doi:10.1016/j.csda.2012.12.008.
- Brechmann, E. C., Czado, C., & Aas, K. (2012). Truncated regular vines in high dimensions with application to financial data. *Canadian Journal of Statistics*, *40*, 68–85. doi:10.1002/cjs.10141.
- Browne, R. P., & McNicholas, P. D. (2015). A mixture of generalized hyperbolic distributions. *Canadian Journal of Statistics*, *43*, 176–198. doi:10.1002/cjs.11246.
- Cabral, C. R. B., Lachos, V. H., & Prates, M. O. (2012). Multivariate mixture modeling using skew-normal independent distributions. *Comput. Stat. Data Anal.*, *56*, 126–142. doi:10.1016/j.csda.2011.06.026.
- Celeux, G., & Govaert, G. (1995). Gaussian parsimonious clustering models. *Pattern Recognition*, *28*, 781 – 793. doi:10.1016/0031-3203(94)00125-6.
- Cuvelier, E., & Fraiture, M. (2005). Clayton copula and mixture decomposition. In *Applied Stochastic Models and Data Analysis (ASMDA 2005)*, Brest, 17-20 May 2005.
- Czado, C. (2019). Analyzing dependent data with vine copulas: A practical guide with R. In *Lecture Notes in Statistics*. doi:10.1007/978-3-030-13785-4_1.
- Dang, U. J., Browne, R. P., & McNicholas, P. D. (2015). Mixtures of multivariate power exponential distributions. *Biometrics*, *71*, 1081–1089. doi:10.1111/biom.12351.
- Dempster, A. P., Laird, N. M., & Rubin, D. B. (1977). Maximum Likelihood from Incomplete Data Via the EM Algorithm. *Journal of the Royal Statistical Society: Series B (Methodological)*, *39*, 1–38. doi:10.1111/j.2517-6161.1977.tb01600.x.
- Dheeru, D., & Karra Taniskidou, E. (2017). UCI Machine Learning Repository. URL: <http://archive.ics.uci.edu/ml>.
- Diday, E., & Vrac, M. (2005). Mixture decomposition of distributions by copulas in the symbolic data analysis framework. *Discrete Applied Mathematics*, *147*, 27 – 41. doi:10.1016/j.dam.2004.06.018.
- Dißmann, J., Brechmann, E. C., Czado, C., & Kurowicka, D. (2013). Selecting and estimating regular vine copulae and application to financial returns. *Computational Statistics and Data Analysis*, *59*, 52 – 69. doi:10.1016/j.csda.2012.08.010.
- Fraley, C., & Raftery, A. E. (1998). How Many Clusters? Which Clustering Method? Answers Via Model-Based Cluster Analysis. *The Computer Journal*, *41*, 578–588. doi:10.1093/comjnl/41.8.578.
- Franczak, B. C., Browne, R. P., & McNicholas, P. D. (2014). Mixtures of shifted asymmetric laplace distributions. *IEEE Transactions on Pattern Analysis and Machine Intelligence*, *36*, 1149–1157. doi:10.1109/TPAMI.2013.216.
- Gambacciani, M., & Paoletta, M. S. (2017). Robust normal mixtures for financial portfolio allocation. *Econometrics and Statistics*, *3*, 91–111. doi:<https://doi.org/10.1016/j.ecosta.2017.02.003>.
- Hartigan, J. A., & Wong, M. A. (1979). Algorithm as 136: A k-means clustering algorithm. *Journal of the Royal Statistical Society. Series C (Applied Statistics)*, *28*, 100–108. doi:10.2307/2346830.
- Hennig, C. (2010). Methods for merging Gaussian mixture components. *Advances in Data Analysis and Classification*, *4*, 3–34. doi:10.1007/s11634-010-0058-3.
- Hu, L. (2006). Dependence patterns across financial markets: a mixed copula approach. *Applied Financial Economics*, *16*, 717–729. doi:10.1080/09603100500426515.
- Joe, H. (1996). Families of m -variate distributions with given margins and $m(m-1)/2$ bivariate dependence parameters. In *Distributions with fixed marginals and related topics* (pp. 120–141). Institute of Mathematical Statistics. doi:10.1214/lnms/1215452614.
- Joe, H. (2014). *Dependence Modeling with Copulas*. New York: Chapman and Hall/CRC. doi:10.1201/b17116.

- Joe, H., & Xu, J. J. (1996). The Estimation Method of Inference Functions for Margins for Multivariate Models. *Technical Report no. 166, Department of Statistics, University of British Columbia*, (pp. 1–21). doi:[10.14288/1.0225985](https://doi.org/10.14288/1.0225985).
- Karlis, D., & Xekalaki, E. (2003). Choosing initial values for the EM algorithm for finite mixtures. *Computational Statistics and Data Analysis*, *41*, 577 – 590. doi:[10.1016/S0167-9473\(02\)00177-9](https://doi.org/10.1016/S0167-9473(02)00177-9).
- Kim, J. M., Kim, D., Liao, S. M., & Jung, Y. S. (2013). Mixture of D-vine copulas for modeling dependence. *Computational Statistics and Data Analysis*, *64*, 1–19. doi:[10.1016/j.csda.2013.02.018](https://doi.org/10.1016/j.csda.2013.02.018).
- Kosmidis, I., & Karlis, D. (2016). Model-based clustering using copulas with applications. *Statistics and Computing*, *26*, 1079–1099. doi:[10.1007/s11222-015-9590-5](https://doi.org/10.1007/s11222-015-9590-5).
- Krupskii, P., & Joe, H. (2013). Factor copula models for multivariate data. *Journal of Multivariate Analysis*, *120*, 85 – 101. doi:[10.1016/j.jmva.2013.05.001](https://doi.org/10.1016/j.jmva.2013.05.001).
- Lee, S., & McLachlan, G. J. (2014). Finite mixtures of multivariate skew t-distributions: Some recent and new results. *Statistics and Computing*, *24*, 181–202. doi:[10.1007/s11222-012-9362-4](https://doi.org/10.1007/s11222-012-9362-4).
- Lin, T. I., Lee, J. C., & Yen, S. Y. (2007). Finite mixture modelling using the skew normal distribution. *Statistica Sinica*, *17*, 909–927. URL: <http://www.jstor.org/stable/24307705>.
- Liu, C., & Rubin, D. B. (1994). The ECME Algorithm: A Simple Extension of EM and ECM with Faster Monotone Convergence. *Biometrika*, *81*, 633–648. doi:[10.2307/2337067](https://doi.org/10.2307/2337067).
- Mangasarian, O. L., Street, W. N., & Wolberg, W. H. (1995). Breast cancer diagnosis and prognosis via linear programming. *Operations Research*, *43*, 570–577. doi:[10.1287/opre.43.4.570](https://doi.org/10.1287/opre.43.4.570).
- Maugis, C., Celeux, G., & Martin-Magniette, M. L. (2009). Variable selection for clustering with gaussian mixture models. *Biometrics*, *65*, 701–709. doi:[10.1111/j.1541-0420.2008.01160.x](https://doi.org/10.1111/j.1541-0420.2008.01160.x).
- McLachlan, G. J., & Peel, D. (2000). *Finite mixture models/Geoffrey McLachlan, David Peel*. Wiley New York; Chichester. doi:[10.1002/0471721182](https://doi.org/10.1002/0471721182).
- McNicholas, P. D. (2016). Model-Based Clustering. *Journal of Classification*, *33*, 331–373. doi:[10.1007/s00357-016-9211-9](https://doi.org/10.1007/s00357-016-9211-9).
- Meng, X.-L., & Rubin, D. B. (1993). Maximum Likelihood Estimation via the ECM Algorithm: A General Framework. *Biometrika*, *80*, 267–278. doi:[10.2307/2337198](https://doi.org/10.2307/2337198).
- Morales-Nápoles, O. (2010). Counting vines. In *Dependence Modeling: Vine Copula Handbook*. doi:[10.1142/9789814299886_0009](https://doi.org/10.1142/9789814299886_0009).
- Murray, P. M., Browne, R. P., & McNicholas, P. D. (2017). A mixture of sdb skew-t factor analyzers. *Econometrics and Statistics*, *3*, 160–168. doi:<https://doi.org/10.1016/j.ecosta.2017.05.001>.
- Nagler, T., Bumann, C., & Czado, C. (2019a). Model selection in sparse high-dimensional vine copula models with an application to portfolio risk. *Journal of Multivariate Analysis*, *172*, 180 – 192. doi:[10.1016/j.jmva.2019.03.004](https://doi.org/10.1016/j.jmva.2019.03.004).
- Nagler, T., Schepsmeier, U., Stoeber, J., Brechmann, E. C., Graeler, B., & Erhardt, T. (2019b). *VineCopula: Statistical Inference of Vine Copulas*. URL: <https://CRAN.R-project.org/package=VineCopula>.
- Panagiotelis, A., Czado, C., & Joe, H. (2012). Pair copula constructions for multivariate Discrete Data. *Journal of the American Statistical Association*, *107*, 1063–1072. doi:[10.1080/01621459.2012.682850](https://doi.org/10.1080/01621459.2012.682850).
- Panagiotelis, A., Czado, C., Joe, H., & Stöber, J. (2017). Model selection for discrete regular vine copulas. *Computational Statistics and Data Analysis*, *106*, 138 – 152. doi:[10.1016/j.csda.2016.09.007](https://doi.org/10.1016/j.csda.2016.09.007).
- Peel, D., & McLachlan, G. J. (2000). Robust mixture modelling using the t distribution. *Statistics and Computing*, *10*, 339–348. doi:[10.1023/A:1008981510081](https://doi.org/10.1023/A:1008981510081).
- Prates, M. O., Cabral, C. R. B., & Lachos, V. H. (2013). mixsmsn: Fitting finite mixture of scale mixture of skew-normal distributions. *Journal of Statistical Software*, *54*, 1–20. URL: <http://www.jstatsoft.org/v54/i12/>.
- R Core Team (2019). *R: A Language and Environment for Statistical Computing*. R Foundation for Statistical Computing Vienna, Austria. URL: <https://www.R-project.org/>.

- Raftery, A. E., & Dean, N. (2006). Variable selection for model-based clustering. *Journal of the American Statistical Association*, *101*, 168–178. doi:[10.1198/016214506000000113](https://doi.org/10.1198/016214506000000113).
- Roy, A., & Parui, S. K. (2014). Pair-copula based mixture models and their application in clustering. *Pattern Recognition*, *47*, 1689–1697. doi:[10.1016/j.patcog.2013.10.004](https://doi.org/10.1016/j.patcog.2013.10.004).
- Sachs, K., Perez, O., Pe'er, D., Lauffenburger, D. A., & Nolan, G. P. (2005). Causal protein-signaling networks derived from multiparameter single-cell data. *Science*, *308*, 523–529. doi:[10.1126/science.1105809](https://doi.org/10.1126/science.1105809).
- Schwarz, G. (1978). Estimating the Dimension of a Model. *The Annals of Statistics*, *6*, 461–464. doi:[10.1214/aos/1176344136](https://doi.org/10.1214/aos/1176344136).
- Scrucca, L., Fop, M., Murphy, T. B., & Raftery, A. E. (2016). Mclust 5: Clustering, classification and density estimation using Gaussian finite mixture models. *R Journal*, *8*, 289–317. doi:[10.32614/rj-2016-021](https://doi.org/10.32614/rj-2016-021).
- Scrucca, L., & Raftery, A. (2015). Improved initialisation of model-based clustering using gaussian hierarchical partitions. *Advances in Data Analysis and Classification*, *9*, 447–460. doi:[10.1007/s11634-015-0220-z](https://doi.org/10.1007/s11634-015-0220-z).
- Sklar, A. (1959). Fonctions de Répartition à n Dimensions et Leurs Marges. *Publications de L'Institut de Statistique de L'Université de Paris*, (pp. 229–231).
- Stöber, J., Joe, H., & Czado, C. (2013). Simplified pair copula constructions—Limitations and extensions. *Journal of Multivariate Analysis*, *119*, 101 – 118. doi:[10.1016/j.jmva.2013.04.014](https://doi.org/10.1016/j.jmva.2013.04.014).
- Sun, M., Konstantelos, I., & Strbac, G. (2017). C-Vine Copula Mixture Model for Clustering of Residential Electrical Load Pattern Data. *IEEE Transactions on Power Systems*, *32*, 2382–2393. doi:[10.1109/TPWRS.2016.2614366](https://doi.org/10.1109/TPWRS.2016.2614366).
- Vrac, M., Chédin, A., & Diday, E. (2005). Clustering a global field of atmospheric profiles by mixture decomposition of copulas. *Journal of Atmospheric and Oceanic Technology*, *22*, 1445–1459. doi:[10.1175/JTECH1795.1](https://doi.org/10.1175/JTECH1795.1).
- Wang, W.-L., & Lin, T.-I. (2015). Robust model-based clustering via mixtures of skew-t distributions with missing information. *Advances in Data Analysis and Classification*, *9*, 423–445. doi:[10.1007/s11634-015-0221-y](https://doi.org/10.1007/s11634-015-0221-y).
- Weiß, G. N., & Scheffer, M. (2015). Mixture pair-copula-constructions. *Journal of Banking & Finance*, *54*, 175–191. doi:[10.1016/j.jbankfin.2015.01.008](https://doi.org/10.1016/j.jbankfin.2015.01.008).
- Zhang, Q., & Shi, X. (2017). A mixture copula bayesian network model for multimodal genomic data. *Cancer Informatics*, *16*, 1176935117702389. doi:[10.1177/1176935117702389](https://doi.org/10.1177/1176935117702389).
- Zhuang, H., Diao, L., & Yi, G. Y. (2021). A bayesian nonparametric mixture model for grouping dependence structures and selecting copula functions. *Econometrics and Statistics*, . doi:<https://doi.org/10.1016/j.ecosta.2021.03.009>.